Åbo Akademi University

Md. Abdullah Al Sazzad

Studies on Ceramide/Colipid Interactions in Complex Bilayers

Biochemistry,
Faculty of Science and Engineering
Åbo Akademi University
Turku, Finland

2017

STUDIES ON CERAMIDE/COLIPID INTERACTIONS IN COMPLEX BILAYERS

Md. Abdullah Al Sazzad

Biochemistry, Faculty of Science and Engineering
Åbo Akademi University
Turku, Finland

2017

Supervised by

Professor J. Peter Slotte

Biochemistry
Faculty of Science and Engineering
Åbo Akademi University
Turku, Finland

Reviewed by

Docent Katariina Öörni
Wihuri Research Institute
Helsinki, Finland

Docent Reijo Käkelä
Department of Bioscience
University of Helsinki
Helsinki, Finland

Opponent

Professor Nobuaki Matsumori

Department of Chemistry
Faculty of Sciences
Kuyshu University
Fukuoka, Japan

ISBN 978-952-12-3614-3
Painosalama Oy – Turku, Finland 2017

To My family

TABLE OF CONTENTS

LIST OF ORIGINAL PUBLICATIONS

This thesis is based on the following original publications referred to by the Roman numerals I-IV throughout the thesis.

I. The Long-Chain Sphingoid Base of Ceramides Determines Their Propensity for Lateral Segregation.
Md. Abdullah Al Sazzad, Tomokazu Yasuda, Michio Murata, and J. Peter Slotte.
Biophysical Journal 112: 976-983, 2017.

II. Influence of Hydroxylation, Chain Length, and Chain Unsaturation on Bilayer Properties of Ceramides.
Terhi Maula, Md. Abdullah Al Sazzad, and J. Peter Slotte.
Biophysical Journal 109: 1639-1651, 2015.

III. Effect of Phosphatidylcholine Unsaturation on the Lateral Segregation of Palmitoyl Ceramide and Palmitoyl Dihydroceramide in Bilayer Membranes.
Md. Abdullah Al Sazzad and J. Peter Slotte.
Langmuir 32: 5973-5980, 2016

IV. The Influence of Hydrogen Bonding on Sphingomyelin/Colipid Interactions in Bilayer Membranes.
Tomokazu Yasuda, Md. Abdullah Al Sazzad, Niklas Z. Jäntti, Olli T. Pentikäinen, and J. Peter Slotte.
Biophysical Journal 110: 431-440, 2016.

CONTRIBUTION OF THE AUTHOR

The author contributions to the publications included in the thesis are as follows:

I. Participated in designing the study together with the supervisor. Performed all the experiments with the exception of the NMR studies which were conducted in Japan. Wrote the manuscript together with the supervisor.

II. Participated in designing the study together with the supervisor and T. Maula. Performed the experiments together with T. Maula. Wrote the manuscript together with the supervisor and T. Maula.

III. Participated in designing the study together with the supervisor. Performed all the experiments. Wrote the manuscript together with the supervisor.

IV. Participated in designing the study together with the supervisor. Performed the experiments together with T. Yasuda. Wrote the manuscript together with the supervisor and T. Yasuda.

Additional publications not included in the thesis

Bilayer Interactions among Unsaturated Phospholipids, Sterols, and Ceramide.
J. Peter Slotte, Tomokazu Yasuda, Oskar Engberg, Md. Abdullah Al Sazzad, Victor Hautala, Thomas K. M. Nyholm, and Michio Murata.
Biophysical Journal 112: 1673-1681, 2017.

Regulation of Sticholysin II-Induced Pore Formation by Lipid Bilayer Composition, Phase State, and Interfacial Properties.
Juan Palacios-Ortega, Sara García-Linares, Mia Åstrand, Md. Abdullah Al Sazzad, José G. Gavilanes, Álvaro Martínez-del-Pozo, and J. Peter Slotte.
Langmuir 32: 3476-3484, 2016.

ACKNOWLEDGEMENTS

The work for this thesis was performed at the Laboratory of Lipid and Membrane Biochemistry, Faculty of Science and Engineering, Åbo Akademi University. During my time (October, 2013 - December, 2017) in the Lipid group I have been lucky to work with many wonderful people. Now I would like to take my chance to express my gratitude to all of you for all the support, science and memorable time.

First, I would like to sincerely thank my supervisor *Professor J. Peter Slotte* for providing me an opportunity to work as a PhD student in his research group. I am privileged to have an excellent supervisor with solid experience in the research field and with great heart. I owe my deepest gratitude to you for your inspiring advice, guidance, understanding and constant support throughout my stay at your lab. Thank you for everything!

I would like to thank all the current and former members of the lipid group specially *Thomas Nyholm, Max Lönnfors, Terhi Maula, Jenny Isaksson, Shishir Jaikishan, Helen Cooper, Oskar Engberg, Henrik Nurmi, Victor Hautala, Anna Möuts and Nozomi Watanabe*. Thank you Thomas for serving as member of my thesis committee. I acknowledge your guidance, being always available for science discussion and especially for all the valuable suggestions during writing process. Thank you Max for helping me out for all the practical issues when I started working in the lipid lab. I thank Terhi for your valuable suggestions and discussions during your stay in the lab. Thank you Oskar for all your cooperation in the lab, science discussion and travel company. It was always enjoyable to me to have the friendly science discussion with you. Thank you Anna especially for helping me in translating Swedish and Finnish. Jenny Isaksson, Shishir Jaikishan and Helen Cooper are acknowledged for your entire positive attitude that was always encouraging for me. Thank you Henrik, Victor, and Nozomi for the great company. Thank you all for the wonderful lunch and coffee breaks with interesting discussions over the years. I would also like to thank all the summer and graduate students that have been in the lab over the years, especially *Anders Kullberg, Mia Åstrand, Niklas Z. Jäntti* and *Toveann Ahlnäs*. Thanks also to the visiting researchers *Tomokasu Yasuda, Nuria Roldán, Sara García Linares* and *Juan Palacios-Ortega*.

I would also like to thank all my coauthors, especially *Professor Michio Murata* and *Professor Olli T. Pentikäinen* for their collaboration. Thank you all the teaching staff and all the people at Biochemistry department. I acknowledge the graduate school ISB, with special thanks to *Mark Johnson* and *Fredrik Karlsson* for organizing wonderful scientific meetings and social activities. I show my deepest gratitude to *Katariina Öörni* and *Reijo Käkelä* for reviewing my thesis. Your constructive criticism and valuable suggestions have improved the standard of the thesis.

I warmly thank all my friends and family living in Finland. They are extremely important for my joyful stay in Finland. Thank you my friend *Munir* & *Oishi* for all your support. Thanks to the Bangladeshi community in Turku specially *Millat vai, Najmul vai, Nasrin vabi, Sajal da, Raju, Sabbir, Sanjib, Rupanti, Khairul, Attiq, Pranjol, and Iqbal*. You all made my days stress free.

I am deeply grateful to my parents, *Md. Mofazzal Hossain* and *Daulatun Nessa* for their love, affection, sacrifice and hard work for making my life bright. I have no words for my parents for being constant source of inspiration. I am deeply obliged to my father whose values towards education and knowledge have been significant in influencing my life. I am also thankful to my parent-in law, my sister *Molly apu* and in-laws. Especial thanks to my uncle *Md. Mobaswar Hossain* (*Sejho kaka*) for always being supportive for me. I must acknowledge my beloved wife *Era* for her continuous support and for being beside me in all circumstances.

I am thankful for the generous financial support received from Academy of Finland, the Magnus Ehrnrooth Foundation, the Foundation of Åbo Akademi University, the Oskar Öflund Foundation, the Medicinska Understödsföreningen Liv och Hälsa r.f., and the Finsk-Norska Medicinska Stiftelsen, and the Sigrid Juselius foundation.

Md. Abdullah Al Sazzad
Turku, 25.10.2017

ABSTRACT

Ceramide belongs to an important class of sphingolipids and it constitutes the hydrophobic backbone of all complex sphingolipids. Ceramide plays an important role in different biological processes such as cell signaling, proliferation, differentiation and apoptosis. Particularly, the role of ceramides in apoptosis has received special attention in recent years. In addition, it is been suggested that the membrane biophysical properties are affected upon generations of ceramide. Therefore, ceramide-related membrane phenomena have become a subject of great interest both in cellular and in model membrane studies. This thesis focuses on investigating how specific structural details of ceramides influence their interactions with other lipids present in the membrane bilayers. The ceramide structure varied with regard to length of both the *N*-acyl chain and long-chain base, interfacial hydroxylation, identity of the headgroup, and the position of cis-double bonds in the chains. We have also examined how the structure of the associated lipids can influence the ceramide-rich phases in bilayer membranes.

Our results demonstrated that structural variation among ceramides leads to differences in their behavior in the membranes. The length of the long-chain base of ceramides had a larger effect on ceramide-colipid interactions compared to the effect of *N*-linked acyl chain length. In addition, the presence of cis-double bonds and their comparative position also caused an important effect on ceramide properties. When we studied how the lateral segregation of ceramides are influenced by the degree of unsaturation of different glycerophospholipids, we observed that these lateral segregations were affected by the overall degree of unsaturation of the sn-2 acyl chain of the PCs. We have also investigated the effect of hydrogen bonding between sphingomyelin (SM) and ceramides or cholesterol interactions. Our findings demonstrated that these interactions are markedly affected by hydrogen bonding properties. Overall, the results of this thesis showed how the gel-phase forming properties of ceramides are influenced by their molecular structure and the colipids present in the membrane bilayers, which may have distinct effects on cell physiology.

ABBREVIATIONS

7SLPC	1-palmitoyl-2-(7-doxyl) stearoyl-*sn*-glycero-3-phosphocholine
C16-cer/ Pcer	N-palmitoyl-D-erythro-sphingosine
C16-phyto-cer	N-palmitoyl-D-erythro-4-hydroxysphinganine
C18(2OH)-cer	N-(2′(R)-hydroxy)-stearoyl-D-erythro-sphingosine
C18:1$^{\Delta 12c}$-cer	N-12Z-octadecenoyl-D-erythro-sphingosine
C18:1$^{\Delta 9c}$ –cer	N-oleoyl-D-erythro-sphingosine
C18-cer	N-stearoyl-D-erythro-sphingosine
C18-sphingadiene-cer	N-stearoyl-D-erythro-sphinga-4E, 14Z-diene
C24:1$^{\Delta 15c}$ –cer	N-nervonoyl-D-erythro-sphingosine
C24-cer	N-lignoceroyl-D-erythro-sphingosine
Cer-1-P	N-palmitoyl-D-erythro-sphingosine-1-phosphate
CTL	Cholesta-5,7,9(11)-trien-3-β-ol, cholestatrienol
DOPC	1,2-dioleoyl-*sn*-glycero-3-phosphocholine
DPG	Dipalmitoylglycerol
DPH	1,6-diphenyl-1,3,5-hexatriene
DPPC	1,2-dipalmitoyl-*sn*-glycero-3-phosphocholine
DSC	Differential scanning calorimetry
OSM	Oleoyl Sphingomyelin
PAPC	1-palmitoyl-2-arachidonoyl-sn-glycero-3-phosphocholine
PC	Phosphatidylcholine
PDPC	1-palmitoyl-2-docosahexaenoyl-sn-glycero-3-phosphocholine
PLPC	1-palmitoyl-2-linoleoyl-sn-glycero-3-phosphocholine
POPC	1-palmitoyl-2-oleoyl-*sn*-glycero-3-phosphocholine
PSM	D-*erythro*-N-palmitoyl-sphingomyelin
SM	Sphingomyelin
T_m	Gel-to-liquid crystalline phase transition temperature
tPA	*trans*-parinaric acid
tPA-Cer	N-*trans*-parinaroyl-D-erythro-sphingosin

1. INTRODUCTION

Cell membranes, which maintain cellular compartmentalization, are one of the most advanced and complex components of cells and have an important role in supporting various cellular events such as cell division, cell–cell communication, signal transduction, and apoptosis. Membranes are highly organized, protect the integrity of the interior organelles of cells, and maintain the cell's shape. The cell membranes are semi-permeable and act as barriers and gatekeepers. This semi-permeable compartmentalization is achieved by the formation of lipid bilayers (Yeagle, 2005). Biological membranes are composed of amphiphilic lipids clustering together to form bilayers; numerous membrane proteins are attached to or embedded within these bilayers. The bilayers are connected to the interior of the cell by a cytoskeleton. On the external side of bilayers, the glycocalyx serves as an area for cell–cell recognition and interactions. In the outer and inner leaflet of plasma membranes, various lipid species are asymmetrically distributed. In plasma membrane, sphingomyelin and phosphatidylcholine are the major constituents of the external leaflet. The membrane's biophysical properties include membrane permeability, membrane fluidity, and membrane curvature, which can all be significantly influenced by the constituent lipids and proteins (Heimburg, 2007). In biological membranes, different sphingolipids together with cholesterol have been involved in lateral domain or 'raft' formation. It has been suggested that lipid rafts have major implications in different cellular processes, such as membrane trafficking, protein sorting and signal transduction (Brown and London, 2000; Simons and Toomre, 2000).

Ceramides, the simplest of all two-chain sphingolipids, are found in very small amounts in cell membranes, but upon accumulation the ceramides may affect cell sensing, apoptosis, and necrosis (Hannun and Luberto, 2002; Obeid et al., 1993). Ceramides have also been implicated in the activation of specific protein phosphatases (Chalfant et al. 2004). It has been observed that the effect of ceramides as modulators of membrane properties are somehow associated with their distinct molecular structure and characteristics, e.g., ceramides are highly hydrophobic, contain very small headgroup, and have high melting temperature. The unique biophysical properties of ceramide led to its ability to induce an increase in molecular ordering and domain formation.

2. REVIEW OF THE LITERATURE

2.1 Biological membranes

Biological membranes are essential components of cells, and they are composed of a lipid bilayer. In the bilayers, the polar headgroups of constituent lipids run along two surfaces and their nonpolar acyl chains lie in between. Many hypotheses regarding the organization of biological membranes and progress in biophysical techniques of membrane research have increased our understanding of the membrane's structural properties. In early twentieth century, Gortel and Grendel (1925) first proposed the structure of biological membranes based on a Langmuir monolayer study. They stated that membrane bilayers contain two layers of amphiphilic molecules and water molecules on both sides of the polar headgroups (Gorter and Grendel, 1925). This view was elaborated further by the for decades accepted membrane model hypothesis, "fluid-mosaic," which was proposed by Singer and Nicolson in 1972; this introduced the foundation of the dynamic nature of lipid–protein interactions in membrane bilayers (Singer and Nicolson, 1972).

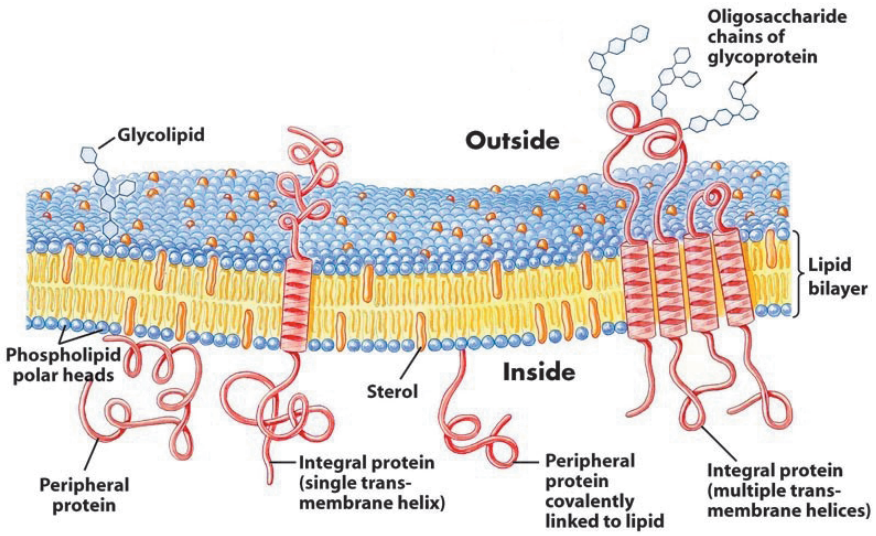

Figure 1. *Schematic representation of the cell membrane and membrane components. Adapted and modified from Nelson, D.L and M.M. Cox, Leninger Principles of Biochemistry, 4th ed., W. H. Freeman, 2005, p.372. © 2005 by W. H Freeman and Company.*

According to the "fluid-mosaic" model, membrane proteins are floating like icebergs in a sea of lipids, and the degree of motion the proteins have significantly impacts their activity. The fluid mosaic model turned out to be a benchmark for our current understanding of membrane bilayer properties and their physiological functions. However, this hypothesis has been revised and updated several times, and it has been proposed that the plasma membrane is not a random ocean of lipids, but rather, there is localized distribution of proteins in dynamic patches of bilayer, called domains. These specific microdomains were named as lipid rafts, which are enriched in sphingolipid-cholesterol and may exist as a distinct liquid-ordered phase (Simons and Ilkonen, 1997). The lateral movement in the bilayers can be restricted because of the presence of lipid rafts; moreover, these microdomains are believed to be involved in different cellular events, such as protein sorting, signal transduction, calcium homeostasis, transcytosis, alternative routes of endocytosis, internalization of toxin, and cholesterol transport (Yeagle, 2005).

Biological membranes consist of diverse lipids, proteins, and carbohydrates. A Schematic representation of the cell membrane and membrane components is shown in Figure 1. In general, biological membranes contain a significant amount of proteins which is almost 50% of the total volume of membranes. Membrane proteins are organized into cell membranes in numerous orientations. Integral proteins are embedded within lipid bilayers, whereas peripheral proteins are associated with membrane surfaces. As for lipid-anchored proteins, they are not directly attached to the membranes; rather, they covalently bind to lipids embedded within the membranes. In addition, the carbohydrate constituents of cell membranes are found on the proteins or lipids protruding outward from the plasma membrane (Luckey, 2008).

2.2 Diversity of membrane lipids and their structure

The diversity of membrane lipids is remarkable. Lipids are typically composed of fatty acids and in lipids the combinations of different fatty acids largely contribute to this structural diversity. More than 1000 different lipids are present in the cellular lipidome (van Meer, 2005). The classification of membrane lipids is arbitrary; they may be classified according to their increasing complexity or based on their functional criteria. In mammalian cell membranes, lipids are classified into three major groups: glycerophospholipids, sphingolipids, and sterols (cholesterol in mammalian

cells). Glycolipids are considered a separate group, even though they are composed of either glycerol or sphingosine backbone containing the mono- or oligosaccharide headgroup. To investigate the properties of biological membranes, it is important to study the behavior of their structural lipid components in the bilayers.

2.2.1 Glycerophospholipids

The most abundant lipid species found in mammalian cell membranes are glycerophospholipids, which are the derivatives of phosphatidic acid. They contain a glycerol backbone where two fatty acids are attached with ester or ether linkages at the position sn-1 and sn-2; a polar phosphate head group is attached at the sn-3 position. Generally, the fatty acid at position sn-1 is saturated, and the other fatty acid at position sn-2 is mono- or polyunsaturated with 1-6 *cis*-double bonds (Dougherty et al., 1987; Barenholz and Thompson, 1999). Among glycerophospholipids, phosphatidylcholine (PC) is the most abundant lipid class found in animals and plants. Molecular structure of the most common PC (1-palmitoyl-2-oleoyl-phosphatidylcholine, POPC) used in our study is presented in Figure 2. The PC species are the key building blocks of membrane bilayers, amounting to almost 50% of the total phospholipids in eukaryotic membranes (van Meer et al., 2008). PC contains the large zwitter-anionic choline head group and two fatty acid acyl chains that are mostly equal in length and make the molecule fairly symmetric. The cylindrical molecular structure of the PC is important for ensuring the formation of membrane bilayers. LysoPC is another class of glycerophospholipid that contains the choline head group and is synthesized from hydrolysis of phosphatidylcholine, catalyzed by the phospholipases A2 (PLA2). The LysoPCs do not form bilayers; rather, they form micelles. Different lysophospholipids are thought to be ligands for different G protein–coupled receptors (GPCRs) (Anlikar and Chun, 2004).

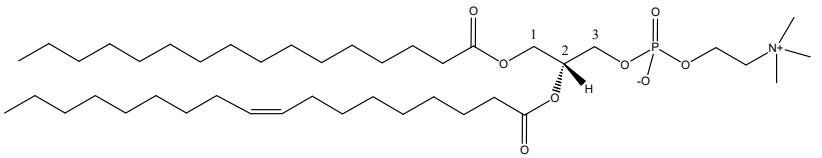

Figure 2. *Molecular structure of the most common PC used in our study*

Phosphatidylethanolamine (PE) is a class of phospholipid which contains a small zwitterionic head group and the acyl chains often have ether linkage. Generally, they are the main lipid component in microbial membranes. Another aminophospholipid found in mammalian cells is phosphatidylserine (PS), generally amounting to less than 10% of the total phospholipids; the concentration of PS is higher in the plasma membranes and endosomes but is found in very low concentration in mitochondria. The PS contains an anionic headgroup and it is the most abundant anionic phospholipid in eukaryotic membranes ((Leventis and Grinstein, 2010).

2.2.2 Sphingolipids

Sphingolipids are the second most abundant class of lipids; they contain the backbone of sphingoid bases. Around 20–25% of the total phospholipid content in the outer leaflet of mammalian plasma membranes are sphingolipids (van Meer et al., 2008). In the late nineteenth century, Johann Thudicum first named sphingolipids after the mythical Egyptian sphinx because of their mysterious structure (Thudicum, 1884). Later, in 1927, the structure of this sphingophospholipid was reported to be *N*-acyl-sphingosine-1-phosphorylcholine (Pick and Bielschowsky, 1927). The structural difference between sphingolipids and glycerophospholipids comes from their hydrophobic region, where sphingolipids contain a sphingoid long chain base to which functional groups and amide-linked acyl chains are attached. In contrast, glycerophospholipids are built on the backbone of L-glycerol. The variations in sphingolipid structures may appear because of differences in the sphingoid base, hydrophilic head groups, or even in acyl chain length.

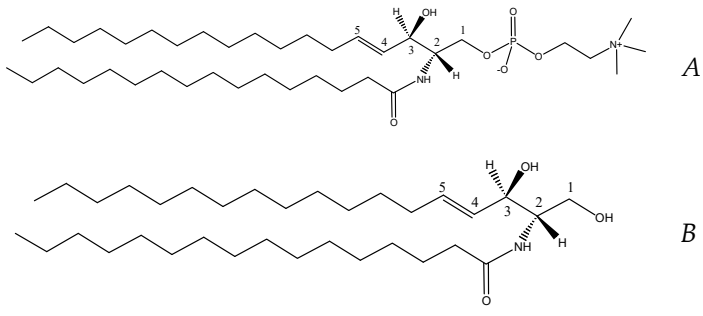

Figure 3. *Molecular structures of palmitoyl-sphingomyelin (A) and palmitoyl-ceramide (B)*

A) Sphingomyelins

Sphingomyelins (SM) are the most ubiquitous sphingolipids in mammalian cells; they contain sphingosine backbone and phosphocholine as a polar headgroup attached to the C1 position. Typically, in natural SMs, the acyl chains are longer than those of PCs. Generally, the saturated acyl chains in natural SMs vary from 16 to 24 carbons in length (O'Brien and Rouser, 1964; Barenholz, 1984). The presence of unsaturation in *N*-linked acyl chains of natural SMs is less common, and if present, the double bonds are found further away from the membrane–water interface (Barenholz, 1984). Even though SMs and PCs contain similar head groups, the structural difference comes from their interfacial region. Sphingomyelins may act as both a donor and accepter of hydrogen bond formation because they contain both an amide- and a 3-hydroxy group, along with carbonyl oxygen, which is linked to the amide; however, PCs can act as acceptors only through the oxygen molecules in their ester linkages (Boggs, 1980; Niemelä et al. 2004). These hydrogen-bonding properties may lead to higher phase transition temperatures in natural SMs compared to natural PCs (reviewed in Ramstedt and Slotte, 2002).

B) Ceramides

Ceramides are the structural precursor of all sphingolipids. They lack a headgroup at the C1 position and contain fatty acids that are attached with an amide linkage to the NH_2 at the C2 position of the long chain base. Pascher proposed the molecular arrangement of ceramides derived from crystal structures, infrared spectra and monolayer studies. In their molecular structure, ceramides contain a rigid amide group with a planar resonance that is perpendicular to the two hydrocarbon chains (Pascher, 1976). Only a hydroxyl group constitutes their small polar head group; therefore, ceramides have less molecular area than SM or PC, and they are highly hydrophobic in nature. Ceramides cannot form a stable bilayer on their own since they are lack of large headgroups, and they depend on other bilayer-forming lipids, such as SM or glycerophospholipids, for bilayer formation (Bonosi et al., 1990).

The structure of ceramides varies widely, and this structural variation arises because of chain-length variations in the acyl chains and sphingoid bases, the degree of unsaturation, and hydroxylation and methylation status. The *N*-acyl

chains of ceramides are mostly saturated and can differ in length between 14 and 36 carbon atoms, as observed in skin ceramides (O'Brien and Rouser, 1964; Fahy et al., 2005; Farwanah et al., 2007). The length of ceramide acyl chains observed in mammalian cells are generally C16–20 and C22–24, whereas ceramides with acyl chain length from C26–36 are observed in epidermal keratinocytes and male germ cells during their differentiation and maturation (Sandhoff, 2010). In mammals, there are six different ceramide synthases (CerS1–6), each of which synthesizes ceramides with distinct acyl chain lengths (Levy and Futarman, 2010). Among these ceramide synthases (CerS1–6), CerS1 mostly synthesizes C18-ceramides (Venkataraman et al., 2002), CerS2 synthesizes ceramides having acyl chain length C20-26 (Laviad et al., 2008), and CerS3 prefers both middle and long-chain acyl-CoA:s (Mizutani et al., 2006; 2008). CerS4 synthesizes ceramide with C18–22 fatty acids, whereas CerS5 and CerS6 synthesize C16 ceramides (Riebeling et al., 2003, Mizutani et al., 2005). However, the length of ceramide sphingoid bases is controlled in the primary stage of *de novo* synthetic pathway through the high selectivity of serine palmitoyltransferases for fatty acyl-CoA:s with 16 ± 1 carbon atoms (Williams et al., 1984; Merrill et al., 1985; Merrill et al.,1988).

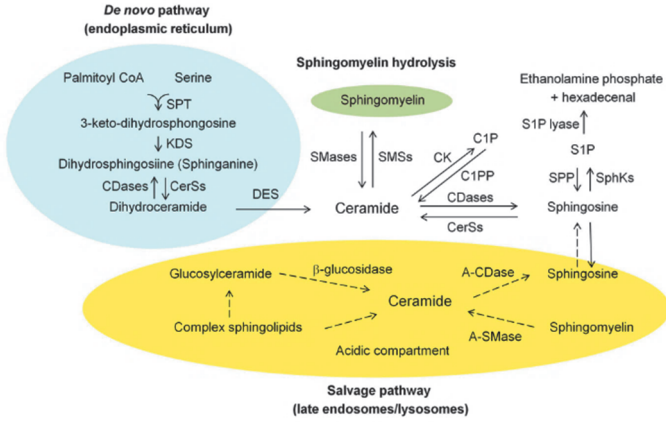

Figure 4. *Metabolism of sphingolipids and major pathways of ceramide synthesis. Adapted from "Ceramide-Induced Apoptosis in Renal Tubular Cells: A Role of Mitochondria and Sphingosine-1-Phoshate" by N. Ueda, 2015, Int. J. Mol. Sci. 16(3): p. 5078. Adopted with permission.*

Ceramides can play a significant role as precursors for more complex sphingolipids. Generally, *de novo* synthesis and salvage pathway are the major pathways of ceramide synthesis (Fig. 4). Synthesis of ceramides in the *de novo*

pathway takes place in the endoplasmic reticulum, where condensation of palmitoyl-CoA occurs with L-serine, leading to the formation of 3-keto-dihydroshingosine (Wu BX et al., 2010; Morad and Cabot, 2013; Carpinteiro et al., 2008; Bartke and Hannun, 2009). In the next step, 3-keto-dihydroshingosine is reduced to dihydrosphingosine, which is later acylated to form dihydroceramide by the action of ceramide synthases (Mullen et al., 2012). Ceramides then need to be transported to the Golgi, where they are converted to higher sphingolipids. This conversion to higher sphingolipids is a very rapid process. Two mechanisms are involved for the transportation: vesicular transport (Watson and Stephens, 2005) and the ceramide transfer protein CERT (Hanada et al., 2007; Yamaoka et al., 2004). SM degradation by sphingomyelinase (SMase) is another way of ceramide generation, and it occurs in the plasma membranes (Gulbins et al., 2004; Airola and Hannun, 2013). SM degradation is known to be the major pathway where cells can generate larger amounts of ceramides quickly. The synthesis of ceramides by the activation of SMases generally occurs within minutes, whereas the biosynthetic route may take hours. In the salvage pathway, which is also known as the sphingolipid recycling pathway, ceramides are generated from the breakdown of complex sphingolipids by activation of hydrolase enzymes (Hannun and Obeid, 2008).

Ceramides are present only in small amounts in cell membranes, about 0.1-1 mol% percent of total phospholipid (Hannun and Obeid, 2011), but the amount may increase with the activation of SMase. Different pro-apoptotic receptor molecules, stress stimuli and viral infections can act as inducers for increasing ceramide levels in cells (Gulbins, 2003; Mathias et al., 1998). Ceramides can act as a key factor for inducing the initiation of apoptosis; higher ceramide level in cells was observed during apoptosis (Hannun, 1996; Hannun and Luberto, 2000). Palmitoyl ceramide was recognized as a probable mediator of death signals while the increased level of other species was not significant (Thomas et al., 1999). In addition to the involvement in apoptosis, ceramides have major implications in different cellular processes such as cell proliferation, migration, differentiation, necrosis, and cytoskeletal rearrangements (Adam et al., 2002; Okazaki et al., 1989; Zhang et al., 1996; Obeid et al., 1993).

A distinct characteristic of ceramides in membrane is that they are able to induce lateral domain formation both in cells (Fanzo et al., 2003) and in model membranes (Nurminen et al., 2002; Carrer and Maggio, 1999; Silva et al., 2006). The formation of these domains may act as a platform for cell-signaling

events. The clustering of such ceramide-rich domains may form larger assemblies (Kolesnick et al., 2000) that can promote the temporary reorganization of membrane components, such as different receptors and signaling molecules, and that can stimulate signal transduction (Stancevic and Kolesnick, 2010). It has also been observed that ceramide-rich domains have been associated with infections by bacteria and viruses (Dreschers et al., 2007; Grassme et al., 2003; 2005; Babiychuk et al., 2009), bacterial mediated hot–cold hemolysis (Montes et al., 2008), and intracellular trafficking (Goldschmidt et al., 2011; Trajkovic et al., 2008). Moreover, ceramides can interact with activated receptors to recruit molecules for transferring the signal and excluding unwanted molecules that may affect signal transduction (Stancevic and Kolesnick, 2010).

It has been reported that ceramides can impact different diseases, such as Alzheimer's disease, cystic fibrosis, renal and liver failure, and tumorigenesis (Zheng et al., 2006; Gulbin and Li PL, 2006). Because ceramides can induce apoptosis, known as programmed cell death, ceramides can inhibit the development and persistence of lung-cancer-derived (Kurinna et al., 2004), colon cancer (García-Barros et al., 2016), and fibrosarcoma tumor cells (Pruschy et al, 1999). Therefore, the role of ceramides could be significant in cancer research (Huang et al., 2011; Reynolds et al., 2004). Ceramides are also observed to interact with different intracellular target enzymes, such as ceramide-activated protein phosphatases 1 (PP1) and 2A (PP2A) (Dobrowsky et al., 1993; Chalfant et al., 1999), protein kinase f (PKCf) (Muller et al., 1995), kinase suppressor of Ras 1 (KSR1) (Zhang 1997), cathepsin D (Heinrich et al.,1999), and Mitogen-activated protein kinase kinase kinase 1 (MEKK1) (Huwiler et al., 2004). Normally, ceramides are restricted to the membrane, and as a result, interacting proteins should translocate to the membrane (Grösch et al., 2011). Ceramides may bind to specific sites of the target proteins and can modulate the enzyme action. In the case of proteins lacking a specific ceramide binding site, ceramides can modify their enzyme activity by altering the physical properties of the membrane's bilayer, because integral or intrinsic membrane proteins are very sensitive to changes in bilayer order or fluidity (Hemminga et al., 1993). In mammalian skin tissue, ceramides play a key role in the formation of the permeability barrier (Norlen et al., 2008; van Smeden et al., 2013).

2.2.3 Sterols

Sterols are other important membrane components mostly found in eukaryotic cell membranes. Compared to the other main lipid classes structural variations in sterols are limited. There are different forms of sterols, but they all contain a common ring structure, the steroid backbone (Yeagle, 2005). Sterols have four fused rings: three of them have six carbon atoms and one has five carbon atoms. Different carbon ring arrangements and difference in the aliphatic side chain can lead to sterol varieties in various organisms. The major sterol found in animal tissue is cholesterol (Fig. 5), the other most abundant sterols found in biological membranes are ergosterol (yeast), stigmasterol, and sitosterol (plant cells).

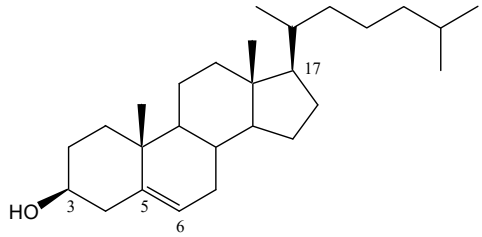

Figure 5. *Molecular structure of cholesterol.*

Cholesterol was first isolated from gallstones in 1789 and was named as "cholesterine" in 1815. Cholesterol on its steroid backbone contains a hydroxyl group at C3, a double bond between C5 and C6, and an iso-octyl hydrocarbon chain that is attached to the steroid nucleus at C17. The rings are fused in all *trans* configuration which makes the molecule flat and rigid with restricted flexibility, except the iso-octyl chain that has some rotational freedom (Yeagle, 2005). In cellular membranes, 40–90% of cholesterol can be found in plasma membranes, whereas the lowest amount is observed in mitochondria and ER (Lange, 1991; Maxfield and van Meer, 2010). All mammalian cells can produce cholesterol, except the red blood cells (RBC). In mammalian cells, cholesterol plays a key role in regulating membrane thickness and membrane fluidity (Rawicz et al., 2008; Hill and Zeidel, 2000; Lande et al., 1995; Hertz and Barenholz, 1975). Cholesterol is also considered to be an essential component in membrane raft formation (Pike, 2006). It has been reported that the lipid rafts have significant influence on cell signaling, cell recognition, and endocytosis. Rafts are also found to be associated with many diseases, such as Alzheimer's disease, prion diseases and different viral infections (Simons and Toomre, 2000; Simons and Ehehalt, 2002). Apart from its role as an important membrane component, cholesterol can also influence the activities of some

membrane proteins involved in membrane trafficking and cell signaling, including the G-protein coupled receptors (Simon and Ikonen, 1997).

2.3 Model membranes and lipid vesicles

In membrane research, model membranes are widely used because they can be designed to mimic biological membranes. Model membranes come in different varieties, and each has its own experimental advantages and disadvantages. Depending on the objective of the experiment, model membranes with specific compositions are commonly used in membrane research. In the current thesis work, synthetically prepared model membrane vesicles of different known lipid compositions were used. In the 1960s, Bangham et al. first introduced lipid vesicles for studying the structural modification of phospholipids (Bangham et al., 1964; 1965). Since then, lipid vesicles have been extensively and efficiently used when studying the properties of membrane lipids. Lipid vesicles are spontaneously formed when dehydrated lipid samples are hydrated (Bangham et al., 1964). In the vesicles, lipid bilayers form a structure that resembles an enclosed spherical shell encapsulated in an aqueous solution; it shows a basic similarity to cellular membranes (Sessa and Weissmann, 1968; Chan and Boxer, 2007). Although sometimes model membrane studies do not provide clear understanding about the complexity of cellular membranes, the use of such model system may partially characterize the lipid interactions. To increase the complexity of model membranes and understand their properties, much effort has been made in membrane research in recent years.

***Figure 6**. Liposomes based on the lamellarity: (A) multilamellar vesicles (MLV) contain many lipid bilayers (B) large unilamellar vesicle (LUV) with a single lipid bilayer (C) small unilamellar vesicles (SUV) that contain a single phospholipid bilayer surrounding the aqueous phase. Adapted from "Liposome and Their Applications in Cancer Therapy" by Pandey et al. 2016, Brazilian Archives of Biology and Technology, 59, e16150477. Adapted with permission.*

In model membrane studies, the preliminary vesicles prepared in an aqueous solution are large multilamellar vesicles. The size of the lipid vesicles may vary and depends on the lipid composition. The size of the small unilamellar vesicles (SUV) may range from 20–100 nm and for large unilamellar vesicles (LUV) it may range from 100–400 nm. In case of multilamellar vesicles (MLV) the size can be 200 nm - 5 μm (Laouini1 et al., 2012). The lateral organization of the lipid bilayers can be affected by the vesicle size they contain; therefore, the size of the vesicle is always considered a significant parameter in model membrane study (Roux et al., 2005; Pencer et al., 2008). Moreover, the different biophysical properties of membrane lipid bilayers, for example, lipid miscibility (Nordlund et al., 1981; Brumm et al., 1996) and the thermodynamic properties and asymmetry of membranes (Nagano et al., 1995; Kucerka et al., 2007) can be influenced by vesicle size as well. In model membrane studies, the preliminary large vesicles need to be broken down in order to reduce the size of the vesicles. Different methods are used to decrease the size and lamellarity of the vesicles; sonication and extrusion are the most frequently used methods (Szoka and Papahadjopoulos, 1980). The size of the vesicles is also strongly affected by the time, intensity, and temperature maintained during sonication (Maulucci et al., 2005; Richardson et al., 2007). Extrusion is another method that can regulate the size of the vesicles in a more reproducible way; this method can produce unilamellar vesicles with a mean size up to 200 nm in diameter (Mayer et al., 1986; MacDonald et al., 1991).

2.4 Aggregations and phase behavior of membrane lipids

Lipids are amphiphilic in nature and contain both polar and nonpolar parts. The polar parts are the headgroups of lipids, which are hydrophilic, and the nonpolar tails; fatty acid acyl chains are hydrophobic. These dual characteristics of lipid components are important for membrane bilayer formation. In biological membranes, the most natural arrangement of phospholipids is the lamellar bilayer, though bilayers may be transiently disrupted and form non-lamellar phases. Lipid polymorphism and the non-lamellar phases also have biological significance in membrane fusion, fission, or vascular transport (Pieter et al., 1986; Marrink et al., 2009).

2.4.1 The hydrophobic effect and lipid aggregation

When lipids come into close contact with water, the hydrogen-bonding network between the water molecules is disrupted, forming a cage around the hydrophobic moiety. It decreases the entropy, which is not a thermodynamically favorable condition. Therefore, to minimize this effect, lipids and the water molecules separate in two phases, reducing the contact between water and the hydrophobic parts of the lipids. This hydrophobic effect is the driving force for lipid aggregation (van Holde et al., 1998; Heimburg, 2007). The form of lipid aggregation in an aqueous solution largely depends on the molecular structure of the lipids. The different orientations of lipid aggregations observed in biological systems are lamellar bilayer, non-lamellar micelles, hexagonal, and inverted hexagonal phases (Yeagle, 2005).

The geometrical configuration of lipids, such as the critical length of the acyl chain (l), headgroup area (a), and acyl chain volume (V), can significantly affect the behavior of lipid aggregation (Barenholz and Thompson, 1999; Israelachvili, 1991). To evaluate the behavior of lipid aggregations in water dispersion, a critical packing parameter (S) is used, defined as the lipid hydrophobic volume (V) divided by the product of the cross-sectional area (a) of the headgroup and the acyl chain length (l), ($S = V/al$). According to this packing parameter, spherical micelles are formed if $S \leq 0.33$, and non-spherical micelles are possible if $0.33 < S \leq 0.5$. Planar bilayers are formed when $0.5 < S \leq 1$, but in case of $S > 1$, an inverted hexagonal structure may appear.

Parameters	*Geometries*	*Representations*
S > 1		
0.33 < S < 0.5		
0.50 < S ≤1		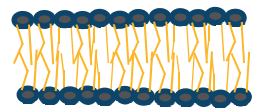

***Figure 7**. Lipid phases (lamellaer or non lameller). Phase formation depends on the molecular geometry of the lipid and can be described by S = V/al.*

In the case of cylindrical-shaped lipids, the packing parameter is close to one, and these lipids form spontaneous lamellar bilayers (Fig. 7). The cone-shaped lipids that contain large headgroups compared to their acyl chain volume (e.g., lysophospholipids, $0.33 < S < 0.5$) are more likely to form micellar structures (Li et al., 2004). They can induce positive membrane curvature (Kooijman et al., 2005). When the size of the lipid headgroup is comparatively small and the packing parameter is over one, the formation of hexagonal phase is promoted, as observed in the presence of ceramides (Veiga et al., 1999). They can induce a negative curvature in the bilayer membranes (Kooijman et al., 2005). Inducing a negative and positive curvature in the bilayers may give rise to membrane tension (Marsh, 1996), which has significant consequences for transmembrane protein activation (Cantor, 1997). However, under some conditions, complex cubic phases may also form apart from the lamellar and non-lamellar phases mentioned above (Tenchov and Koynova, 2012).

2.4.2 Thermotropic transition of lipid phases

The phase behavior of membrane bilayers largely depends on some external factors, such as temperature, hydration, ionic strength, pressure, and pH. Among these external factors, the temperature-dependent phase behavior of membranes has been the most widely investigated. Diverse types of lamellar phases may exist in the membrane bilayer, such as a gel phase (L_β), ripple phase ($P_{\beta'}$), liquid disordered phase (L_d), and liquid ordered phase (L_o). A series of different phases (Fig. 8) is observed with an increase in temperature (Janiak et al., 1979).

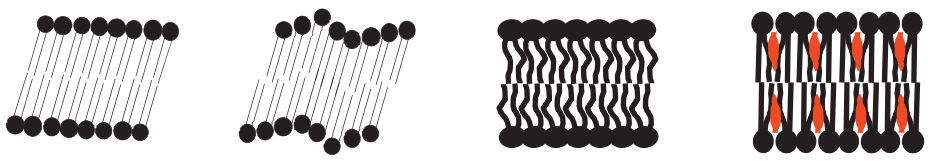

gel-state phase ($L_{\beta'}$)

ripple phase ($P_{\beta'}$)

liquid disordered phase (L_d)

liquid ordered phase (L_o), Cholesterol is shown in red

Figure 8. *Schematic representation of the different lipid phases*

At lower temperatures, bilayers usually remain in the gel or solid ordered phase and in this phase; the acyl chains of the bilayer lipids are extended and arranged in a highly ordered all-*trans* configuration (Heimburg 2007; Huang et al, 1999a). In the gel phase, the cross-sectional area of the lipid molecules is minimal, causing maximal thickness of the bilayers, and both the intra- and intermolecular motion in the bilayers is severely restricted (McMullen et al., 1995). An increase in temperature leads to a decrease in the *trans-gauche* ratio in the acyl chains; as a result, the ordered acyl chains become more fluid, and they go through a gel-to ripple and then ripple-to-fluid phase transition. In the ripple phase the periodic arrangements of gel and fluid phase exists simultaneously (De Vries et al., 2005).

In the liquid disordered phase, the molecular motion of the lipids increases in the bilayers, and the acyl chain tails lose their tilted positions. The polar headgroups and the interface region of the hydrophobic acyl chains become more hydrated by the surrounding water molecules. The gauche conformations in the acyl chains increase, consequently leading to an increase in the cross-sectional area for lipid molecules. Therefore, the bilayers are laterally enlarged, which causes a decrease in bilayer thickness (Heimburg, 2007; Huang et al., 1999a). Lipid bilayers are in the liquid disordered (L_d) phase above the T_m of the lipids, where the molecular motions are relatively higher compared to the ordered phase. Generally, unsaturated PCs have a lower T_m (below 0℃) than SMs; (between 40–50℃) because of the presence of a higher degree of saturation in the acyl chains, hence providing stronger van der Waals interactions. Even if there are double bonds present in the acyl chains of the SMs, they are usually further away from the membrane–water interface than those in the acyl chains of PCs (Koynova and Caffrey, 1995; 1998). The length of the acyl chains also affects the T_m of the lipids; both the PC and SM show a curvy-linear relationship between T_m and the number of acyl chains.

Cholesterol can significantly regulate the biophysical properties of phospholipid bilayers by inducing a new phase known as the liquid ordered phase (L_o). The liquid ordered phase (L_o) shows the properties that lie between the gel phase (L_β) and the liquid disordered phase (L_d) (Vist and Davis, 1990; Kahya et al., 2003). When cholesterol is introduced in the phospholipid bilayers, the sterol rings promote interactions between the acyl chains that increase the effective chain length but decrease the acyl chain volume in the bilayers. As a result, the thickness of the bilayer membrane increases where acyl chains are more densely packed.

Moreover, the phase behavior of complex lipid mixtures also largely depends on the interactions among constituent lipids in addition to external physical factors. The chemical and physical properties of the individual lipids of a lipid mixture can affect the lipid–lipid interaction and their phase behavior in membrane bilayers. These interactions could be due to different electrostatic interactions, such as ionic interaction, van der Waals interactions, charge pair, and hydrogen bonds.

2.5 Membrane biophysical properties of ceramides

The membrane properties of ceramides depend on their molecular structure. Because of their unique structural properties, ceramides are highly hydrophobic, have a high T_m, and show restricted miscibility with other lipids (Jendrasiak and Smith, 2001; Chen et al., 2000; Westerlund et al., 2010; Sot et al., 2005). Ceramides contain a sphingoid long-chain base or sphingosine to which mostly saturated acyl chains are *N*-linked. It has been shown that the double bond observed between the C4 and C5 position of ceramides contributes to their membrane-packing properties (Brockman et al., 2004). The saturated acyl chains of ceramides may form strong van der Waals interactions with neighboring saturated lipids; meanwhile, their sphingosine backbone can act both as a donor and acceptor in hydrogen bond formation. Shah et al. first suggested that ceramides may form a hydrogen bonding network with their neighboring ceramides; the hydroxyl hydrogen of sphingosine form a bond with the amide group of neighboring ceramides (Shah et al, 1995). However, recent results obtained from molecular dynamic simulation by Pandit et al. showed this is not the amide group; rather it is the carbonyl oxygen that would bind to the hydroxyl hydrogen (Pandit and Scott, 2006). Some major biophysical properties of membranes that can be influenced by ceramides are described in the following sections.

2.5.1 Ceramide-induced ordering of phospholipid bilayers

Ceramides tend to have two important effects on fluid phospholipid membrane bilayers (Castro et al., 2014). They increase the order of the fluid membranes (Huang et al., 1996; 1998; Holopainen et al. 1997; 1998) and induce phase separation in the bilayers (Carrer and Maggio, 1999; Silva et al., 2006). Holopainen et al. reported that C16-ceramide increases the acyl chain order

of both DMPC and POPC bilayers (Holopainen et al., 1997). Moreover, studies using ^{2}H-NMR spectroscopy confirmed that the acyl chain order parameters of DPPC and POPC in a fluid state significantly increased in the presence of both bovine brain ceramide and synthetic C16-ceramide (Huang et al., 1996; 1998, Hsueh et al., 2002). Since ceramides increase the order of the phospholipid bilayers, they lead to a lateral phase separation in the fluid membranes. Incorporation of ceramide in the fluid phospholipid bilayer causes lateral phase separation into gel and liquid phase regions, where ceramides tend to partition into the gel phase (Huang et al., 1996; 1998). Because ceramides can form extensive hydrogen bonding networks with other membrane lipids and have high T_m, ceramides may cause phase coexistence. A slight increase in the amount of ceramides can lead to dramatic changes in the membrane's biophysical properties, and the effect also largely depends on the different ceramide species present in the bilayers. Pinto et al. showed the effect of different saturated and unsaturated ceramides in POPC bilayers; they demonstrated that saturated ceramides (C16, C18, and C24) were more efficient to induce ordered gel phase formation than unsaturated ceramides (C18:1, C24:1) (Pinto et al., 2011).

2.5.2 Formation of ceramide-rich domains in membranes

The lateral phase separation of ceramides can lead to the formation of ceramide-enriched micro-domains. Huang et al. first demonstrated the presence of such domains in phospholipid bilayers by conducting ^{2}H-NMR studies, where they reported ceramide-enriched micro-domains in the DPPC bilayers (Huang et al., 1998). Later ceramide-induced micro domain formation was also reported in dimyristoyl-PC bilayers (Huang et al., 1998, Lehtonen et al., 1996). Ceramide-induced lateral segregation and gel domain formation in fluid POPC bilayers has also been demonstrated by different methods (Silva et al., 2006; Huang et al., 1998; Hsueh et al., 2002; Fidorra et al., 2006). Silva and coworkers first reported the phase diagram for a POPC/Pcer system (Silva et al., 2006). According to their phase diagram, at low ceramide concentrations and higher temperatures, spherical vesicles in the fluid phase dominated, whereas decreasing the temperature led to the coexistence of the fluid and ceramide-rich gel phases and eventually the coexistence of the POPC-rich and ceramide-rich gel phases. Increasing ceramide concentrations above 50 mol%, showed a highly ordered new ceramide-rich phase. Additionally, ceramide-enriched ordered domains were also distinguished in bilayers containing SM/ceramide vesicles (Sot et al., 2006). Sot et al. described the presence of such

domains using fluorescence microscopy in giant unilamellar vesicles (GUVs) containing SM and ceramides. Their results showed that vesicles with pure SM were stained quite uniformly while the presence of ceramides on such vesicles led to the formation of rigid domains, even at lower ceramide concentrations, as indicated by the dark regions in GUVs. Fairly similar results were obtained from a mixture containing bovine brain-SM/bovine brain-Cer (Massey, 2001) and C16-SM/C16-Cer (Busto et al., 2009).

Moreover, the effect of ceramides on more complex membrane bilayers containing ternary or quaternary model membranes was investigated; ceramides showed a higher affinity for ordered domains in the membranes (Wang and Silvius, 2003). It was observed in a ternary mixture containing POPC/C16-SM/C19-Cer (Castro et al., 2007) and POPC/egg-SM/C16-Cer (Boulgaropoulos et al., 2011) bilayers that ceramides can form a SM/ceramide-rich gel phase domain. According to the phase diagram of these ternary mixtures, SM/ceramide-rich gel phase domains can coexist with the POPC-rich fluid phase, depending on the lipid composition (Castro et al., 2007; Boulgaropoulos et al., 2011).

2.5.3 Membrane structural reorganization promoted by ceramides

In addition to induced biophysical changes in the membrane bilayers, ceramides can promote membrane structural and morphological reorganization. Ceramides induce negative curvature in the leaflet where they exist and are generated (Veiga et al., 1999; Kolensnick et al., 2000). This curvature effect occurs due to the molecular geometry of ceramides as they contain a small polar head group and large hydrophobic volume. The effect of negative curvatures in membranes induced by ceramides, may promote the lamellar-hexagonal transition (Sot et al., 2005), membrane fusion (Holopainen et al., 1997), and vesical budding (Ruiz-Arguello et al., 1998). Ceramide-induced non-lamellar phase formation was observed in bilayers containing PE phospholipids (Ruiz-Arguello et al., 1996), whereas the effect was not apparent in the absence of PE (Holopainen et al., 2000; Silva et al., 2006; Castro et al., 2007; Pinto et al., 2011). Ruiz-Arguello et al. described membrane permeability upon ceramide accumulation in membrane bilayers where they reported on ceramide-induced vesicle leakage and aggregation (Ruiz-Arguello et al., 1996; 1998).

Barbosa-Barros et al. showed that ceramides promote the size alteration, morphology, and bilayer thickness of the bicelles composed of DMPC/DHPC and this promotion depends on the nature and concentration of the ceramides (Barbosa-Barros et al., 2008). Ceramide-induced morphological alterations and aggregation was also demonstrated by Silva et al. in POPC bilayers; they showed the formation of cylindrical and crystalline structures at higher ceramide content of 50 mol % and 92 mol%, respectively, in POPC bilayers (Silva et al., 2006). Pinto et al. studied the effect of *N*-acyl chain length on the ceramide gel phase domain and demonstrated that different *N*-acyl chain ceramides segregate into gel domains with distinct properties and shapes (Pinto et al., 2008; 2011). According to their results, the size of the gel domains decreases as the acyl chain length of the saturated ceramides increases. The morphologies of ceramide domains were different: C16-cer segregated into "flower-like" shape domains, and C18- and C24-cer elongated into round-shaped domains. Interestingly, very long chains of ceramides promoted the formation of tubular structures in membrane bilayers. This could be explained by the inter-digitation of very long chains of ceramides, where long acyl chains may enter into the opposite bilayers (Pinto et al., 2008; 2011).

2.5.4 Ceramide and cholesterol interplay in membrane bilayers

In general, cholesterol increases the order of a disordered phase but creates a disordering effect in an ordered phase. Despite ceramide and cholesterol do not form stable bilayers of their own they can form bilayers in presence of PC or SM, and therefore the interplay between ceramides and cholesterol has been of great interest in membrane research over the past years. Megha and London first reported that ceramides displace cholesterol from the L_o domain of a saturated PC bilayer (Megha and London, 2004). Alanko et al. showed the displacement of cholesterol from SM/Cer-rich ordered domains in POPC bilayers, where ceramides showed a high affinity for PSM to form the gel phase (Alanko et al., 2005).

Regarding ceramide-induced cholesterol displacement from a PSM-rich domain, Nybond et al. proposed that ceramides must have at least eight carbons to promote this displacing effect (Nybond et al., 2005). Megha and coworkers also showed the ceramide chain length dependent displacing effect on cholesterol from an SM-rich ordered domain (Megha et al., 2007). These studies indicated that short chain ceramides (<C8-C12) are less capable of displacing cholesterol from SM-rich domains; meanwhile, intermediate- and

long-chain ceramides are more effective. Ali et al. showed that the displacing effect of ceramide can occur with a 1:1 stoichiometry (Ali et al., 2006). When the cholesterol concentration is very high, it can dissolve the ceramide-rich gel domain in fluid bilayers (Castro et al., 2009). Staneva et al. reported a higher miscibility of ceramides with a cholesterol-rich fluid membrane (Staneva et al., 2009). Silva et al. also observed in POPC/PSM/Chol bilayers that the ceramide/SM gel phase domains were formed at a lower cholesterol content, whereas the ability of ceramide to form a gel domain decreased with the inclusion of cholesterol (Silva et al., 2009). A recent study by Slotte et al. showed that in PC/Cer/Chol bilayers, the effect of cholesterol on the ceramide-rich gel phase was also markedly influenced by the acyl chain composition of fluid PCs (Slotte et al., 2017). Busto et al. studied the interaction of ceramides and cholesterol in the absence of the L_d phase in a bilayer containing SM/Chol/Cer; they observed that Cer-cholesterol interaction may depends on both the concentration of ceramide and cholesterol (Busto et al., 2010). Altogether, two common phenomena were observed from these studies: (i) ceramides have the ability to displace cholesterol from a highly ordered gel phase and (ii) lateral segregation of ceramides in the presence of cholesterol mainly depends on the concentration of cholesterol in the membrane; at low cholesterol concentrations, ceramides can still form ceramide-rich ordered domains, but at high cholesterol content, ceramide-rich domain formation may be abolished by the cholesterol.

3. AIMS OF THE STUDIES

The main aims of the current thesis were to investigate how the structural difference among ceramides may affect their molecular properties and their interactions with colipids in membranes and to understand how the properties of a ceramide-rich phase can be affected by the characteristics of the associated lipids present in bilayer membranes. The specific aims of each original publication are listed below.

In **paper I**, the aim was to understand how the lateral segregation of ceramides in a fluid phospholipid bilayer is affected by the length of both the sphingoid base and the *N*-linked acyl chain of ceramides. We systematically examined the lateral segregation and thermostability of a series of saturated ceramides with variable long-chain bases and acyl chain lengths in POPC bilayers.

In **paper II**, the aim was to study how the structural variation of ceramides may lead to alterations in their membrane bilayer properties. This structural variation could arise from the difference in the length of *N*-linked acyl chains, interfacial hydroxylation, and identity of head group and position of *cis*-double bonds in the acyl chains. We examined the bilayer properties of different naturally occurring ceramides in mixed bilayers together with PSM, POPC, and cholesterol.

In **paper III**, the aim was to investigate the interactions of saturated ceramides with unsaturated glycerophospholipids in bilayer membranes to understand how the ceramide properties are influenced in the membrane bilayer by increasing the unsaturation of glycerophospholipids. We examined the lateral segregation of palmitoyl ceramide (Pcer) and fully saturated dihydro-Pcer in an increasingly unsaturated phosphatidylcholine (PCs) bilayer. The PCs used in this study were 16:0/18:1 (POPC), 16:0/18:2 (PLPC), 16:0/20:4 (PAPC), and 16:0/22:6 (PDPC). We also included di-18:1-PC (DOPC) to compare it with POPC.

In **paper IV**, the aim was to study the effect of hydrogen bonding on sphingomyelin (SM) and colipid interactions in fluid membrane. In this study, ceramides and cholesterol were used as colipids, and their interactions in the SM and dihydro-SM bilayers were examined to evaluate the influence of hydrogen bonding because the hydrogen-bonding properties of SM and dihydro-SM differ.

4. MATERIALS AND METHODS

The materials and methods are described in full detail in their respective papers (I-IV). Only a brief description of the experimental approaches and parameters are presented here.

TABLE 1. Experimental approaches and parameters examined in the original publications (I-IV).

Experimental approaches	***parameters examined***	***Paper***
Fluorescence anisotropy	*Membrane order, end-point temperature of the gel-phase melting*	*I–IV*
CTL quenching	*Sterol-rich domain formation, sterol displacement*	*II*
tPA lifetime	*Membrane order, domain properties, phase coexistence*	*I-IV*
CTL-partitioning	*Sterol affinity for bilayers*	*IV*
Differential scanning calorimetry (DSC)	*Lipid mixing, phase behavior*	*II, III*
Nuclear magnetic resonance	*Membrane order*	*I*
Computational simulation	*Molecular properties and interaction*	*IV*

The model membrane vesicles used for our studies were prepared either by sonication that yielded mostly multi-lamellar vesicles or by extrusion that generated mostly unilameller vesicles. For fluorescence experiments, vesicles were prepared with the indicated (mentioned in associated papers, I-IV) concentration of desired lipid composition and fluorophores. The molecular structures of the fluorescent probes and the quencher lipids used in our studies are presented in Figure 9. Structural analogs of ceramides were synthesized either in our laboratory (I–IV) or in the laboratory of Professor Michio Murata (I). Fluorescence anisotropy was performed to study the ceramides-induced membrane order and to detect the end-point temperature of the gel-phase melting of the membrane bilayers. In addition to this,

differential scanning calorimetry (DSC) was used to investigate the lipid-mixing properties and phase behavior of the bilayer membranes. To study the formation and properties of sterol containing membrane domain, CTL quenching experiments were performed.

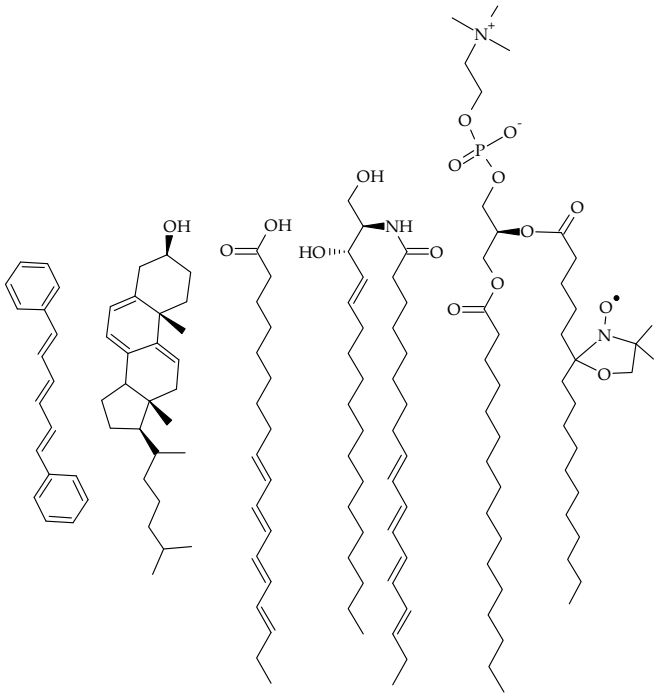

Figure 9. *Molecular structures of the fluorescent probes and the quencher lipid used in this thesis (from left to right): diphenylhexatrien (DPH), cholestatrienol (CTL), trans-parinaric acid (tPA), trans-parinaroyl-ceramide (tPA-Cer), and the spin-labeled quencher lipid (7SLPC).*

Also, the fluorescence lifetime analysis of tPA and tPA-Cer were performed to study the lateral segregations and phase behavior of ceramides in membrane bilayers. Nuclear magnetic resonance (NMR) experiments were performed in the laboratory of Professor Michio Murata to detect the ceramides-promoted ordered phase in the fluid bilayers (I). To study the molecular structure and the interacting properties of SM, computational simulation was performed in the laboratory of Professor Olli Pentikäinen (IV).

5. RESULTS AND DISCUSSION

5.1 Lateral segregation of ceramides is mostly determined by their long-chain sphingoid base

Ceramides contain a long-chain sphingoid base to which a fatty acyl moiety is amide (*N*)-linked (Barenholz and Thompson, 1980). Similar to the acyl chains of the ceramides, the length and nature of the sphingoid long-chain base may also differ in various tissues and organisms (Pruett et al., 2008). To understand how the length of the long-chain base or the *N*-linked acyl chain of ceramides affects their bilayer properties, we examined the lateral segregation of a set of saturated ceramides with variable long-chain bases and acyl chain lengths in POPC bilayers. The long-chain base ceramides used in this study were d16:1, d17:1, d18:1, d19:1, and d20:1 in *N*-palmitoyl ceramides and the acyl chain ceramide analogs were sphingosine (d18:1)-based ceramides with *N*-linked acyl chains of increasing length (14:0 and 16:0–20:0 in one-carbon increments).

5.1.1 Lateral segregation of ceramide analogs in POPC bilayers

The POPC bilayers containing an increasing amount of ceramide analogs with different long-chain bases and different acyl chain lengths were prepared to study their lateral segregations. Lifetime analysis of *trans*-parinaric acid (tPA) fluorescence was performed at 23°C to determine the lateral segregations and ceramide-rich phase formation in POPC bilayers. In tPA lifetime experiments, the time-resolved fluorescence decay component of tPA in a mixture, indicates the packing properties of the mixture. Because tPA shows a higher affinity for the ordered phases in the bilayers (Sklar et al., 1979), it is a very efficient fluorescence probe to detect the lateral segregation and ceramide-rich phase formation. The lifetime component of tPA fluorescence significantly increases when it partitions into an ordered or ceramide-rich phase from a disordered phase (Ekman et al., 2015; Silva et al., 2007).

Our results showed that the intensity weighted average lifetime of tPA increased as the amount of ceramides increased in the bilayers (Fig. 10), which is an indication of more ordered phase formation. We observed that less ceramides were needed for the onset of lateral segregation and ceramide-rich phase formation, with the increasing length of long-chain bases (d16:1, d17:1, d18:1, d19:1, and d20:1 in *N*-palmitoyl ceramide). Among the long-chain base ceramide analogs, 20:1-Pcer containing the longest long-chain base formed a

ceramide-rich phase at the lowest ceramide concentration above 2.5 mol% (Fig. 10A). A clear effect of chain length dependent lateral segregation of the long-chain base ceramide analogs were observed from the tPA lifetime analysis. When we examined the effect of the *N*-linked acyl chain length on the lateral segregation of d18:1-based ceramide analogs, we observed similar trend but smaller difference in the aggregation propensity among the ceramides having different acyl chain length (Fig. 10B). The *N*-linked acyl chain ceramide analogs formed ceramide-rich phases with very similar packing properties, which was observed from the similar longest lifetime component of tPA fluorescence (Paper I, Fig. 2B).

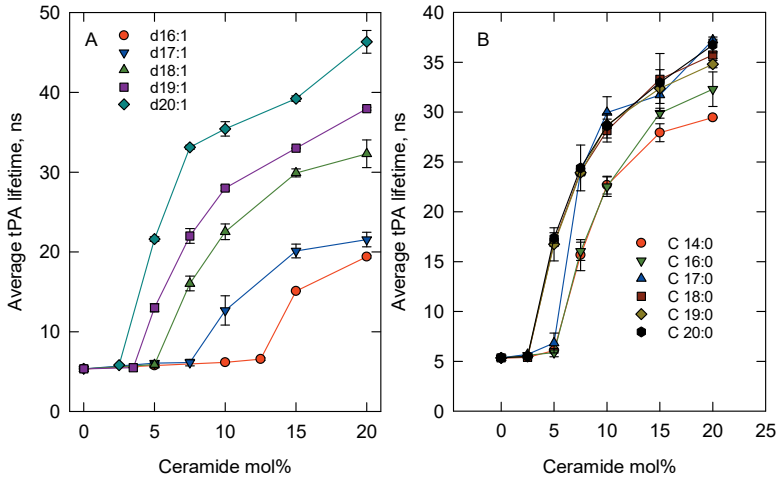

Figure 10. *Lateral segregation of ceramide analogs in POPC bilayers at 23°C. Intensity weighted average lifetime of tPA fluorescence in bilayers was measured as a function of ceramide concentration. (A) Long-chain base analogs, (B) acyl chain analogs. Each value is the average ± SEM; n = 2–3; ns, nanoseconds. The figure is adapted from paper I with the permission of Elsevier.*

5.1.2 Gel-phase thermostability of ceramide analogs in POPC bilayers

The thermostability of ceramide-rich phases of ceramide analogs in POPC bilayers was studied at 1:9 ceramide/POPC molar ratio. Steady-state fluorescence anisotropy of tPA-Cer was performed as a function of temperature to detect the end temperature of ceramide-rich phase melting. We observed that for both types of ceramide analogs (long-chain base and acyl chain analogs), the thermal stability in the POPC bilayers increased with increasing chain length (Fig. 11). However, the length of the long-chain base

in palmitoyl ceramides showed a larger effect on ceramide-rich phase stability compared to d18:1-based ceramides with *N*-linked acyl chains varying from 14:0 to 20:0 (Fig. 11).

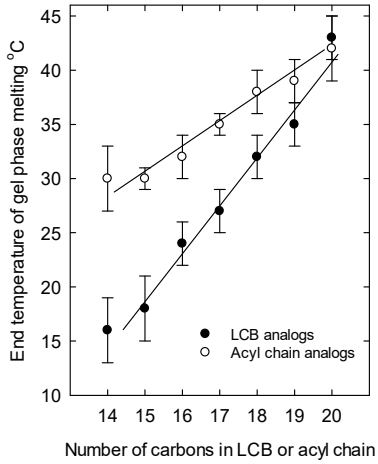

Figure 11. *End melting temperature of the ceramides/POPC phase as a function of long-chain base or acyl chain length. The POPC bilayers contained 10 mol% ceramide analog, and the end temperature of the melting of the ceramide-rich phase was determined from tPA-Cer anisotropy measurements. Each value is the average ± SEM from n=2–3. LCB, long-chain base. The figure is adapted from paper I with the permission of Elsevier.*

The end temperature for the gel phase melting of ceramide acyl chain analogs varied approximately from 30 to 41°C, whereas for long-chain base ceramide analogs the temperature varied approximately from 16 to 43°C. The results obtained from tPA-Cer fluorescence anisotropy measurements were in agreement with our tPA fluorescence lifetime analysis (Fig. 10), where a larger effect was also observed in the case of the ceramide long-chain base analogs on their lateral segregation and ceramide-rich phase formation.

5.1.3 Properties of ceramide asymmetric analogs in fluid bilayers

In addition, we also studied the behavior of two asymmetric ceramide analogs that had an equal number of carbons in the chains (sum of carbons in long-chain base and acyl chain=33) but differing chain lengths (d20:1/13:0 and d16:1/17:0, Fig. 12A) to compare the effect of the long-chain base and the *N*-linked acyl chain on their lateral segregation and ceramide-rich phase stability. Our results from the tPA lifetime analysis showed that the onset of

lateral segregation of the ceramide-rich phase occurred earlier for the ceramide analog with a longer long-chain base.

In POPC bilayers, d20:1/13:0 ceramides segregated into the ceramide-rich phase at a lower concentration of ceramides (>7 mol%) compared to d16:1/17:0 ceramides (~12.5 mol%, Fig. 12B), which had the shorter long-chain base of the two analogs. When we compared the thermostability of these asymmetric ceramide analogs in POPC bilayers using tPA anisotropy, we observed that d20:1/13:0 ceramide was more thermostable compared to d16:1/17:0 ceramide (Fig. 12C). Therefore, our results indicated that the effect of a long-chain base length was more prominent on ceramide-rich gel phase formation and gel phase thermostability compared to acyl chain length.

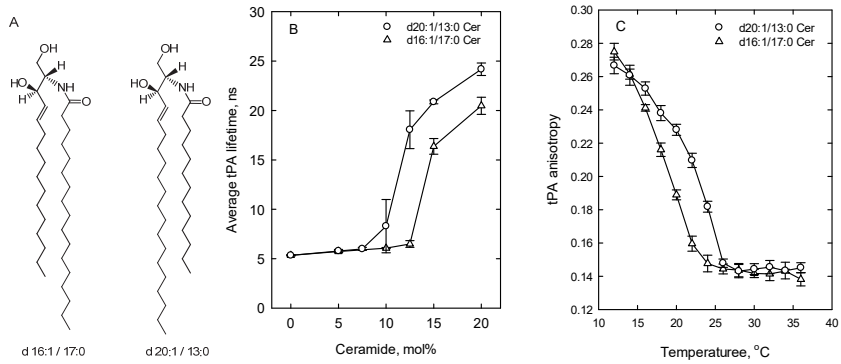

Figure 12. *Effect of asymmetric analogs of ceramide on lateral segregation and gel-phase thermostability in POPC bilayers, as determined by tPA fluorescence lifetime analysis and anisotropy. The ceramide analogs had either a long-chain base of d16:1 or d20:1, or an N-linked acyl chain of 17:0 or 13:0. (A) Chemical structure of the two ceramide analogs. (B) Intensity-weighted average lifetime of tPA fluorescence. (C) Thermostability of the ceramide-rich gel phase based on tPA anisotropy measurements. The composition in (C) was 10 mol % ceramide analog in POPC. Each value is the average ± SEM; n = 3; ns, nanoseconds. The figure is adapted from paper I with the permission of Elsevier.*

To further verify the behavior of asymmetric ceramide analogs in POPC bilayers, ^{2}H NMR measurements were performed. We measured the long-chain base or acyl chain order in site-deuterated d18:1/18:0 ceramides and compared the quadrupolar splitting value ($\Delta\nu$) of 12,12- d_2-labeled long-chain base and 10′,10′- d_2-labeled stearoyl chain as a function of temperature. In SM bilayer, it has been reported that the 12 position on the long-chain base resides at the same depth as the 10′ position on a stearoyl chain (Matsumori et al., 2012).

We observed that in the temperature range of 20-30°C, the quadrupolar splitting values (Δν) were considerably higher for the 12,12-d_2 carbon of the long-chain base than for the 10′,10′- d_2-carbon of the stearoyl moiety (Fig. 13). The difference in quadrupolar splitting values (Δν) disappeared as the temperature increased. Similar (Δν) values at 35°C or above that temperature indicated that the mobility (^{2}H Pake splitting) of the two chains of ceramide became similar. However, different behavior was observed for SM analogs in POPC bilayers (Paper I, Fig. S6).

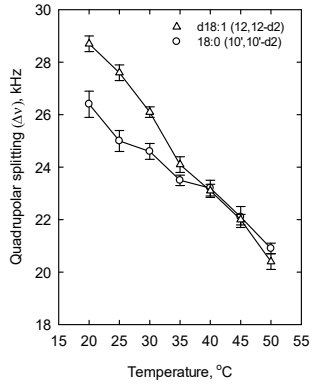

Figure 13. *Order profile of site-deuterated long-chain base or acyl chain in stearoyl ceramide. In the ceramide, either the sphingosine long-chain base was site-deuterated (d_2) at carbon 12, or the stearoyl acyl chain at carbon 10. The quadrupolar splitting* (Δν) *was determined as a function of temperature for the two ceramide analogs. The ceramide content was 10 mol % in POPC. Each value is the average ± SEM; n=2. The figure is adapted from paper I with the permission of Elsevier.*

It has been previously reported that the saturated ceramides laterally segregate into ceramide-rich gel phase in fluid phospholipid bilayers (Carrer and Maggio, 1999; Veiga et al., 1999; Ali et al., 2006; Silva et al., 2006; 2007, Castro et al., 2007; Ekman et al., 2015). To some extent, this lateral segregation is due to the absence of a large headgroup in the ceramides that could protect their hydrophobic parts from interfacial water (Ali et al., 2006; Huang, 1999b; 1999c). Another possible reason for the lateral segregation of saturated ceramides is to avoid interactions with disordered acyl chains and favor interactions with saturated acyl chains (Paper III). For the stabilization of ceramide gel phases, hydrogen bonding involving the 2-NH appeared to be important (Maula et al., 2011, Ekman et al., 2015), and the 1-OH is also likely to be involved in interfacial hydrogen bonding. It has been observed that the lateral segregation of ceramide analogs are not affected by the methylation of 3-OH; therefore, the 3-OH involved in hydrogen bonding may not be very critical (Ekman et al., 2015).

To our knowledge, there are no reports on comparative studies of the effects of long-chain base length and acyl chain length on ceramide behavior in unsaturated phospholipid bilayers. Fyrst et al. who characterized *Drosophila melanogaster* ceramide analogs with variable length long-chain bases, reported significant differences in biophysical properties for sphingolipids having short-chain sphingoid bases and long-chain sphingoid bases (Fyrst et al., 2004). The effects of long-chain base length of ceramides were examined previously on ceramide-SM interactions and it was observed that the thermostability of equimolar ceramide/SM mixed bilayers was markedly influenced by the long-chain base length of ceramides (Maula et al., 2012). However, we did not observe any notable influence of the acyl chain length on the thermostability of equimolar ceramide/SM mixed bilayers containing saturated C16-, C18- and C24-ceramides (Fig. 15). In POPC bilayers, we found that the long-chain base length of ceramides had a more dramatic effect on their lateral segregation into gel phase (Fig. 10) and on the thermostability of ceramide rich gel phase (Fig. 11).

Our results indicate that the interactions of the ceramide analogs with POPC are asymmetric, and this evidence was further supported by the results obtained from asymmetric ceramide analogs (d20:1/13:0 or d16:1/17:0). Higher gel-phase thermostability was observed for the ceramide analog with a longer sphingoid base (Fig. 12C) and also a higher chain order (quadrupole splitting) was detected in the sphingoid base than in the acyl chain at comparable deuteron positions and temperatures (Fig. 13). We think these asymmetric interactions are possible for two reasons: (i) because POPC is a hybrid lipid (Heberle et al., 2013), a saturated colipid prefers to interact with the palmitoyl residue rather than with the oleoyl residue of POPC; and (ii) since the intermolecular interactions were more strongly affected by the long-chain base than acyl chain length, apparently the ceramides interacted with the palmitoyl residue of POPC mainly via the long-chain base, not so much via the saturated *N*-linked acyl chain. Such asymmetric interactions are likely to involve the orientation effects caused by favorable hydrogen bonding between the ceramides and POPC, since the long-chain base of ceramides contains two hydrogen-bond donating and accepting functional groups (1-OH and 3-OH), whereas the *N*-linked acyl chain contains a hydrogen-bond accepting group (carbonyl ester oxygen) and the NH, which can donate hydrogen for intermolecular interactions.

5.2 Effect of hydroxylation, chain length, and chain unsaturation on ceramide-rich domain formation

In addition to variations in the length and nature of the sphingoid long-chain base, the structural diversity in ceramides may also arise due to variations in the length of their *N*-linked acyl chains, with the different level of unsaturation, hydroxylation, and branching that may occur at different positions on the *N*-linked chain (Fahy et al., 2005). To study the influence of specific structural aspects on the bilayer properties of ceramides, we examined the properties of different biologically relevant ceramides in mixed bilayers together with PSM, POPC, and cholesterol. Ceramides used in this study were saturated C16-, C18- and C24-ceramides, ceramide-1-phosphate, and monounsaturated C18:1$^{\Delta 9c}$ and C24:1$^{\Delta 15c}$ species, all containing the sphingosine (18:1$^{\Delta 4t}$) long-chain base. The two hydroxylated ceramides used were C18^{2OH}-ceramide, i.e., the (2'R)-isomer of the α-hydroxylated ceramides with a sphingosine long-chain base and C16-phytoceramide with the (4'R)-hydroxy sphinganine long-chain base. In addition, to compare the effect of the *cis*-double bond present in the long-chain base and in the *N*-acyl chain, ceramides containing an unsaturated sphingadiene long-chain base (C 18:2$^{\Delta 4t, 14c}$) and ceramides with an unsaturated C18:1$^{\Delta 12c}$ *N*-linked acyl chain were also included. The molecular structures of the ceramides used in this study are presented in Figure 14.

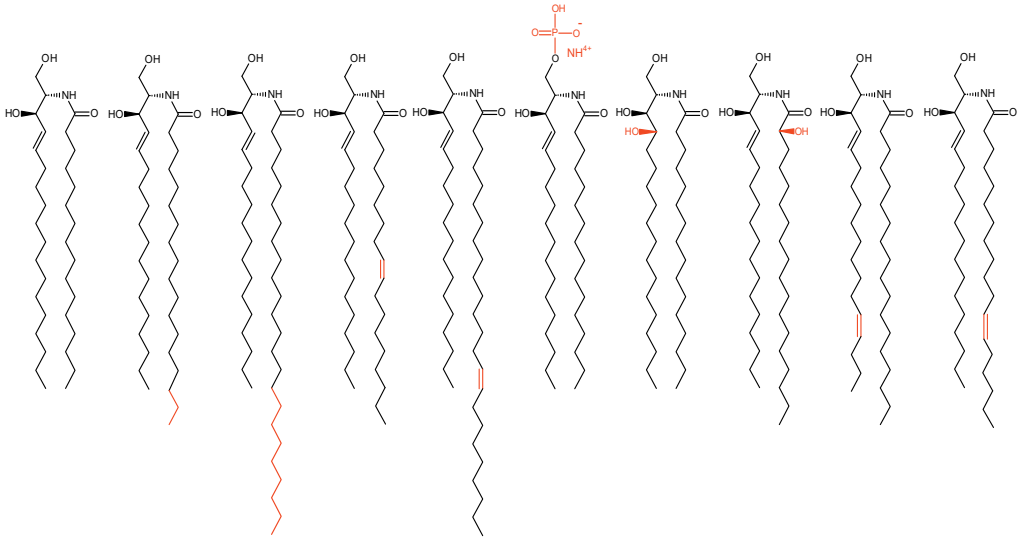

Figure.14. Molecular structures of (from left to right) C16-cer, C18-cer, C24-cer, C18:1$^{\Delta 9c}$-cer, C24:1$^{\Delta 15c}$-cer, Cer-1-P, C16-phytocer, C18^{2OH}-cer, C18-sphingadienecer, and C18:1$^{\Delta 12c}$-cer.

5.2.1 Effect of saturated *N*-acyl chain length

To study the influence of ceramides' structure on their bilayer properties, we examined the interactions of ceramides with PSM in binary mixtures of ceramides/PSM (1:1) using DSC experiments (Fig. 15). Increasing the ceramide *N*-acyl chain length from C16 to C18 or C24 showed very small variations in the T_m as pure components had a range from 91 to 93°C (Westerlund et al., 2010; Jime´nez-Rojo et al., 2014). Similarly, when these ceramides were mixed with PSM, no major differences in the main T_m were observed (Fig. 15). Only a slightly lower T_m was observed in the presence of C18-cer and C24-cer compared to C16-cer; although, as a pure component, C16-cer showed the lowest T_m among these ceramides. Possibly, this effect was due to a larger hydrophobic mismatch that led to lower molecular packing and a lower degree of interactions. Similar behavior was also observed with various binary mixtures of SMs and ceramides with different *N*-acyl chain lengths in monolayer studies (Dupuy and Maggio, 2014). With the increase of the ceramide chain lengths, an increase in the complexity of bilayer phase transition was observed, which was demonstrated by the broadening of the transition peaks. The mixture containing C24-cer/PSM showed a more complex and broad transition that may have resulted from chain interdigitation.

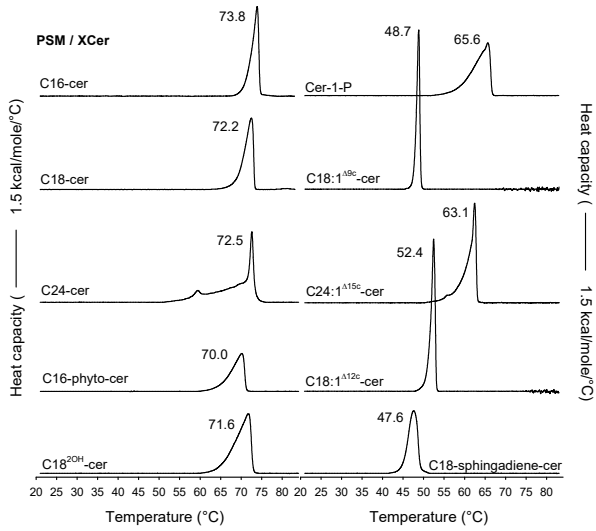

Figure 15. *DSC thermograms of binary ceramides-PSM bilayers. Representative thermograms of the 6th heating scans (1°C/min) of equimolar binary mixtures (1 mM) of the ceramides and PSM from two independently repeated experiments are shown. The T_m for the main (highest) transition peak is given for each mixture. The figure is adapted from paper II with the permission of Elsevier.*

The properties of ceramides were also investigated in binary mixtures with POPC and ternary mixtures with POPC/PSM using steady-state anisotropy and lifetime analysis of tPA fluorescence. In POPC/Cer mixtures, the ceramides gel phase melting temperatures increased with *N*-acyl chain length (obtained from tPA anisotropy Fig. 16), though little variation was observed in the fluorescence lifetime (Fig. 17). It indicates that in the POPC bilayer, even though the thermal stability of the ceramide-rich gel phase was affected by the *N*-acyl chain length, the average degree of acyl chain packing in the bilayers was almost unaffected. These results are in agreement with our observations (in Paper I) where the differences in *N*-acyl length of ceramide analogs did not show any significant effect on their lateral segregations in POPC bilayers. The presence of PSM on the ceramide-rich phase in the POPC bilayer increased the membrane order, as indicated by the increasing gel phase melting temperature and lifetime components.

5.2.2 Effect of interfacial hydroxylation and phosphate headgroup

To detect the effect of interfacial hydroxylation and modification of the ceramide C1 hydroxyl (by a phosphate headgroup), C16-phyto-cer, C18^{2OH}-cer, and Cer-1-P were included. According to the DSC thermograms, the binary C16-phyto-cer/PSM mixture displayed a lower (~4°C) transition temperature compared to the C16-cer/PSM mixture (Fig. 15). It has been reported previously that as a pure component, a phytosphingosine backbone containing ceramides and SMs shows higher gel-to-fluid transition temperatures than analogous sphingolipids with a sphingosine backbone (Rerek et al., 2001; Jaikishan and Slotte, 2013). However, it has also been shown in both monolayer (Lofgren and Pascher, 1977) and infrared studies (Rerek et al., 2001) that phytosphingosine chains are less tightly packed than sphingosine chains. This characteristic of phytosphingosine chains is closely related to our observation, where the transition temperature of the C16-cer/PSM mixture was higher than the C16-phyto-cer/PSM mixture. It indicates that in the C16-phyto-cer/PSM mixture, the destabilizing effect due to looser chain packing of C16-phyto-cer is more prominent than the stabilizing effect of an enhanced H-bonding capacity.

Results from tPA anisotropy reported similar gel phase melting temperatures for C16-cer and the chain equivalent C16-phyto-cer in POPC bilayers in the absence and presence of PSM (Fig. 16). Therefore, the effect of additional hydroxylation in thermal stability was not apparent in the POPC bilayers,

although a clear reduction in the transition temperature of the C16-phyto-cer/PSM mixtures was observed (Fig. 15). However, tPA lifetime analysis reported a significantly lower degree of bilayer order and the packing order for C16-phytocer compared to C16-cer, both in the absence and presence of PSM (Fig. 17). This could be associated with the previous observation that phytosphingosine chains displayed a lower degree of packing properties (Rerek et al., 2001, Lofgren and Pascher, 1977). Interestingly, the presence of PSM noticeably increased the packing order of C16-phyto-cer containing bilayers as observed from increased tPA lifetime component (Fig. 17).

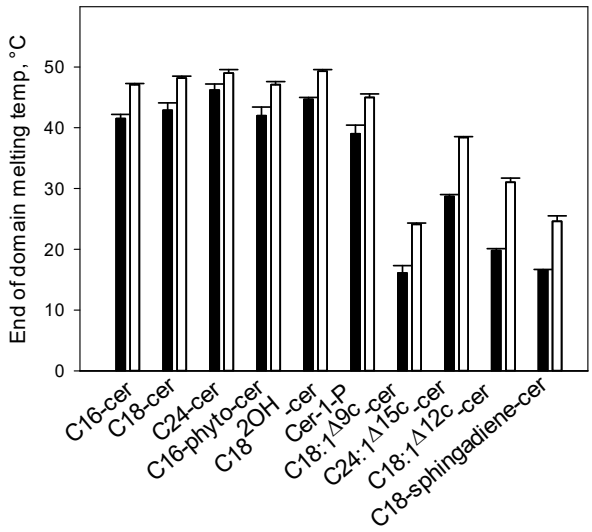

Figure 16. *End-point temperature for ceramide-rich domains in various mixed bilayers containing binary POPC/XCer-60:15 (Solid bar) and ternary POPC/PSM/XCer-60:15:15 (Open bar). The values were deduced from measurements of tPA (1 mol %) fluorescence anisotropy as a function of increasing temperature. Each value is the mean + SEM for n=3. The figure is adapted from paper II with the permission of Elsevier.*

The presence of α hydroxylation (C2-OH) on the *N*-acyl chain of SM also showed a higher T_m as a pure component compared to nonhydroxylated SM (Ekholm et al., 2011). Enhanced molecular packing due to α-hydroxylation in ceramides was also observed compared to their nonhydroxylated counterparts (Pascher, 1976). However, the binary mixture with PSM hydroxylated ceramides $C18^{2OH}$ -cer showed almost a similar (<1°C difference) T_m to the chain equivalent C18-cer (Fig. 15), demonstrating that stabilization of intermolecular interactions by the α-hydroxylation was not apparent in a

binary mixture of an α-hydroxylated ceramides and a nonhydroxylated SM. Though, the presence of an additional hydroxyl in C18^{2OH}-cer slightly increased the gel phase melting temperature (Fig. 16) and degree of packing order in POPC bilayers (Fig. 17) compared to C18-cer both in the absence and presence of PSM. PSM increased the thermal stabilization of the bilayers, inducing an increased fraction of ordered lipids (Fig. 16), but no apparent effect was observed in the degree of bilayer order (Fig. 17).

When we examined the effect of the phosphate headgroup, Cer-1-P showed very different biophysical properties from the chain-matched C16-cer. Because Cer-1-P has a highly polar phosphate head group, as a pure component, it is able to form a bilayer on its own, which contrasts ceramides (Kooijman et al., 2008). As a pure component, the T_m of Cer-1-P (~65°C (Kooijman et al., 2008)) is significantly lower compared to C16-cer (~90°C (Shah et al., 1995; Sot et al., 2005)). Our results also showed a significantly lower T_m for the binary mixture of PSM/Cer-1-P than with the chain-equivalent C16-cer (Fig. 15). The DSC thermogram showed a broader transition peak, which is indicative of a complex gel phase transition and poor miscibility with PSM. This could be explained by the repulsion of the head group within Cer-1-P that subsequently reduced its lateral chain packing.

Interestingly, Cer-1-P displayed a comparatively high gel phase melting temperature both in the absence and presence of PSM in the POPC bilayers; the melting temperature was only a few degrees lower than the chain-equivalent C16-cer. However, clear differences in the packing properties of these ceramides were observed from the tPA lifetime data, where Cer-1-P showed a lower degree of packing order than C16-cer both in the presence and absence of PSM (Fig.17). Our results indicated that the phosphate head group in Cer-1-P obviously restricted the chain interactions, resulting in lower degree lateral packing and (slightly) reduced thermal stability compared to C16-cer in the POPC bilayer.

5.2.3 Effect of an unsaturated *N*-acyl chain and long-chain base

In the case of the unsaturated ceramides, the binary mixtures in PSM displayed lower T_m values than their saturated counterparts. The presence of *cis*-double bonds in acyl chains may perturb the chain packing and, subsequently, can reduce the gel-to-fluid transition temperature of lipids in a position-dependent way (Marsh, 1999). *Cis*-double bonds increase the lateral

space requirement of the molecules, and the presence of *cis*-unsaturation affects the packing properties of ceramides in a position-dependent manner. In the PSM bilayers, C18:1$^{\Delta 9c}$-cer showed a lower T_m than C24:1$^{\Delta 15c}$-cer, which is a clear indication of the position-dependent effect of *cis*-unsaturations. In C18:1$^{\Delta 9c}$-cer, the double bond is in the middle region of the *N*-acyl chains, whereas in C24:1$^{\Delta 15c}$-cer, the double bond is closer to the membrane's hydrophobic core, next to the distal end of the sphingoid base where the disruption in chain packing is less dramatic (Lofgren and Pascher, 1977).

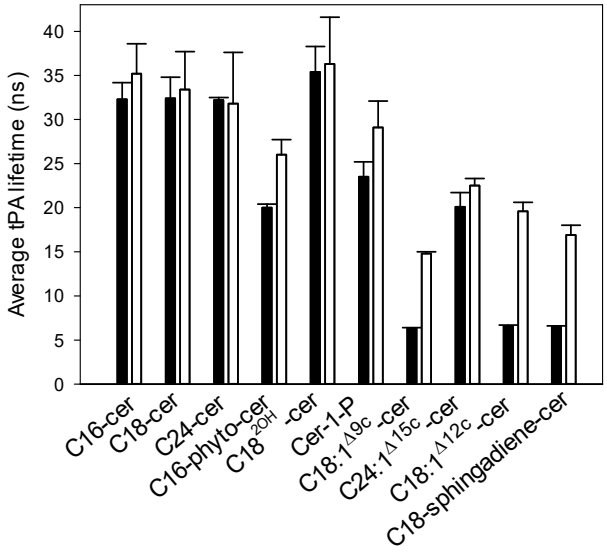

Figure 17. *Fluorescence lifetimes of tPA in various mixed bilayers. The average lifetime of tPA (1 mol%) in binary POPC/XCer 60:15 (Solid bar) and ternary POPC/PSM/XCer 60:15:15 (Open bar). Each value is the average from at least three independently repeated experiments. The figure is adapted from paper II with the permission of Elsevier.*

Also, in C18:1$^{\Delta 12c}$-cer, the presence of a *cis*-double bond resulted in a lower T_m in the binary mixture compared to saturated C18-cer, though this effect was slightly smaller than for C18:1$^{\Delta 9c}$-cer (Fig. 15). This behavior again indicates the position-dependent effect of *cis*-double bonds. Interestingly, the presence of a *cis*-double bond in a sphingoid base of C18-sphingadiene-cer showed a larger decrease in the T_m of the binary mixture than for C18:1$^{\Delta 12c}$-cer, where the *cis*-double bond in the acyl chains is approximately a similar bilayer depth. Moreover, the binary C18-sphingadiene-cer/PSM mixture showed less cooperativity in the melting transition than the C18:1$^{\Delta 12c}$-cer/PSM mixture. This is a clear indication that the double bond in the sphingoid base of

ceramides has a higher impact on the ceramides' properties in the PSM bilayer. Perhaps the *cis*-double bond introduced in the sphingoid base orientationally changed the C4 trans-double bond, which is a key factor in ceramides acyl chain packing (Lofgren and Pascher, 1977; Brockman et al., 2004) and is also thought to have an important role in the intermolecular H-bonding network within ceramides (Brockman et al., 2004, Li et al., 2002).

In the POPC bilayers, binary mixtures of the unsaturated ceramides showed significantly lower points of gel phase melting temperatures than for the other ceramides (obtained from tPA anisotropy analysis; Fig. 16). This observation also reflects the position-dependent effect of unsaturations on acyl chain packing and is in agreement with the DSC experiment (Fig. 15). Among the unsaturated ceramides, the thermostability of the ceramide-rich phases was higher in C24:1$^{\Delta 15c}$-cer, followed by C18:1$^{\Delta 12c}$-cer- and C18:1$^{\Delta 9c}$-cer. The effect of the unsaturation of the sphingoid base was more prominent than the unsaturation of the *N*-acyl chain, where the binary mixtures containing C18-sphingadiene-cer showed lower thermostability than C18:1$^{\Delta 12c}$-cer. A similar effect was observed for the binary PSM/Cer mixtures (Fig. 15)

Results from tPA lifetime in the binary mixtures showed that among the unsaturated ceramides, only C24:1$^{\Delta 15c}$-cer induced a ceramide-rich ordered phase at 23°C, and all other mixtures displayed significantly lower lifetimes, indicating the presence of a fluid phase in the bilayers (Fig. 17). This observation was in line with the anisotropy data, where only the C24:1$^{\Delta 15c}$-cer binary mixture showed a phase melting temperature above 23°C, while all other mixtures were below 23°C (Fig. 16). The addition of PSM in the binary mixtures increased the order of the bilayers observed from both tPA-anisotropy (Fig. 16) and lifetime data (Fig. 17).

Altogether our results show that the domains formed by the saturated and hydroxylated ceramides in POPC bilayers have considerably higher degrees of chain packing and thermal stability compared to unsaturated species. Moreover, differences in bilayer properties of saturated ceramides due to interfacial hydroxylation or variation in the acyl chain length are smaller than differences within different unsaturated species. Similar behavior in membrane properties was reported due to differences in ceramide acyl chain length and unsaturation (Pinto et al., 2011). Also in PSM bilayers, the gel phase melting temperatures for saturated and hydroxylated ceramides are higher than the unsaturated ceramides. These results are in agreement with a previous study by Dupuy and Maggio, where using monolayer studies they

reported that the phase behavior of ceramide-SM mixtures mainly depends on their acyl chain order (Dupuy and Maggio, 2014). We found that the addition of PSM in the binary mixture increased the packing order and the thermostability of the bilayers. Also results obtained from the DSC experiment demonstrated that all the ceramides used in our study interacted favorably with PSM. This observation further supports the evidence that ceramides show a high affinity for ordered domains (Wang and Silvius, 2003). The properties of the unsaturated ceramides were significantly influenced by the relative position of the *cis*-double bond. The effect of unsaturation was more prominant when the double bond is located on the midpart of the *N-acyl* chain. Marsh et al. reported a similar position dependent effect of unsaturation on acyl chain packing in glycerophospholipids (Marsh, 1999). Presence of a *cis*-double bond introduces the destabilization effect by decreasing the van der Waal's interactions between lipid acyl chains (Koynova and Caffrey, 1998). Our results also displayed that the presence of a double bond in the sphingoid base shows higher impact on biophysical properties of ceramides in membranes than a double bond present in the *N-acyl* chain.

5.2.4 Effect of cholesterol on ceramide-PSM rich domains

We investigated the effect of cholesterol on ceramide-PSM rich domains using tPA anisotropy, tPA lifetime, and CTL quenching. The fluorescence CTL quenching was a very efficient method for this study, because CTL partitions only in sterol-rich domains but not in ceramide-PSM rich domains. CTL is a cholesterol-mimicking probe. Therefore, in CTL quenching method the absence of a detectable melting of sterol-rich domain point out the displacement of the probe from the domain into POPC-rich fluid phase where it is quenched by the fluid quencher lipid (Alanko et al., 2005, Bjorkqvist et al., 2005). In our CTL quenching assay (Fig. 18), curves showing a detectable melting point indicate the presence of cholesterol-rich domains whereas linear graphs are signifying the absence of cholesterol-rich domains.

Like ceramide, cholesterol also showed favorable interactions with saturated SMs and were able to form the SM/cholesterol-rich ordered phases (Marsh, 2009; de Almeida et al., 2003). Since both the ceramides and cholesterol have the tendency to interact with SM, their presence in the same bilayer was interesting to study, because there was the possibility they would compete to interact with SM. Depending on the membrane composition, ceramides and

cholesterol display subsequent influences on each other: at a low cholesterol level, ceramides displace cholesterol from the ordered phase, and at a high cholesterol level, cholesterol induces destabilization and solubilization of ceramide-rich phases (Silva et al., 2007; Castro et al., 2009; Pinto et al., 2013). Moreover, SM, cholesterol, and ceramides sometimes coexist to form a ternary phase in the absence of a fluid phase (Busto et al., 2010; 2014).

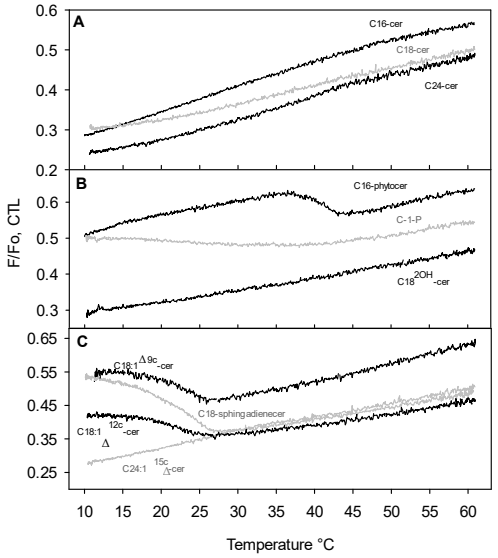

Figure 18. *Quenching of CTL fluorescence in quaternary mixture bilayers containing the ceramides with varying acyl chain lengths (A), interfacial hydroxyl groups or phosphate head group (B), and unsaturated chains (C). The 7SLPC-induced quenching of CTL fluorescence was measured in the F-samples (7SLPC/POPC/PSM/XCer/Chol/CTL; 30/30/15/15/9/1 by mol) and the Fo-samples (POPC/PSM/XCer/Chol/CTL; 60/15/15/9/1 by mol). F/Fo thus denotes the fraction of unquenched CTL fluorescence as a function of increasing temperature. Representative quenching curves from at least three independently repeated experiments are shown for each mixture. The figure is adapted from paper II with the permission of Elsevier.*

Our results obtained from tPA anisotropy showed that saturated ceramides (C16-, C18-, and C24-cer) in ternary POPC/PSM/Cer mixtures displayed domain end-melting around 47- 49°C. When cholesterol was incorporated, the quaternary POPC/PSM/Cer/Chol mixtures showed domain end-melting around 44°C, which is few degrees lower than the end-melting of the mixtures in the absence of cholesterol (Paper II, Table 2). At 23°C, tPA average lifetime revealed similar lateral-packing properties of these domains (Paper II, Fig 2C), though domain disorder was observed to some extent by the increased acyl chain mismatch (Paper II, Fig. 3 left panel). CTL quenching did not show any

sterol-rich domain melting, though cholesterol was present in these bilayers (Fig. 18A), which is a clear indication that cholesterol was not incorporated into these ceramide-PSM rich domains.

The presence of cholesterol on hydroxylated ceramides and Cer-1-P-rich domains influenced these bilayers differently (Fig. 18B). An efficient displacement of cholesterol occurred in the case of C18^{2OH}-cer, though C16-phyto-cer was unable to displace cholesterol from the ceramide-PSM rich domains. In addition, no evidence of sterol-enriched domain melting was observed in the presence of Cer-1-P; however, a gradual decrease of F/F_o was apparent over the temperature range (10 - 40°C). These results indicate that cholesterol was incorporated to a small or a large extent into ordered domains in the presence of Cer-1-P and C16-phyto-cer. Among the unsaturated ceramides, only C24:1$^{\Delta 15c}$-cer displaced cholesterol from the ordered domains (Fig. 18C). For the other unsaturated ceramides, clear domain melting was observed with the CTL-quenching assay (Fig. 18C), indicating strong cholesterol incorporation into the ordered domains of these bilayers.

5.3 Effect of phosphatidylcholine unsaturation on the lateral segregation of ceramides

The lateral segregation of ceramides in fluid bilayers has been widely investigated (Ekman et al., 2015; Hsueh et al., 2002, Pinto et al., 2011, Silva et al., 2007; Sot et al., 2005; Veiga et al., 1999). We have also shown how the lateral segregation and ceramide-rich phase formation of different ceramides in POPC bilayers are influenced by their structural properties, particularly long-chain base properties and acyl chain properties (length and unsaturation). To our knowledge, there are no reports on how the properties of ceramides may be affected by increasingly unsaturated glycerophospholipids in membrane bilayers. Because various types of glycerophospholipids with different level of unsaturation in their acyl chains are present in biological membranes, we think it is important to study how this difference in glycerophospholipids unsaturation can affect the properties of ceramides. The effect of increasing unsaturation in glycerophospholipids has been studied to some extent in the case of glycerophospholipid, cholesterol, and sphingomyelin miscibility (Kullberg et al., 2015; Brzustowicz et al., 2002; Shaikh et al., 2009; Soni et al., 2008, Williams et al., 2012). The objective of our project was to investigate how the lateral segregation of palmitoyl ceramide (Pcer) and the fully saturated dihydro-Pcer can be

affected by increasingly unsaturated PCs. In our investigation, we used the unsaturated PCs with a palmitoyl residue at sn-1 and one of the following acyl chains: 18:1, 18:2, 20:4, or 22:6 (POPC, PLPC, PAPC, and PDPC, respectively) at the sn-2 position. We also included DOPC as a dimonounsaturated PC to compare it with POPC.

5.3.1 Lateral segregation of ceramides in increasingly unsaturated PC bilayers

The lifetime analysis of tPA fluorescence was performed to detect the concentration-dependent lateral segregation of Pcer and dihydro-Pcer in increasingly unsaturated PXPC bilayers (with PXPC being POPC, PLPC, PAPC, or PDPC). To detect the ceramide-rich ordered phase formation in a fluid bilayer, tPA lifetime analysis is a sensitive method since tPA favorably partition into the ceramide-rich phase, and with the increase of more ordered ceramide-rich phase formation, the fluorescence lifetime of tPA increases (Silva et al., 2006; Ekman et al., 2015, Hsueh et al., 2002).

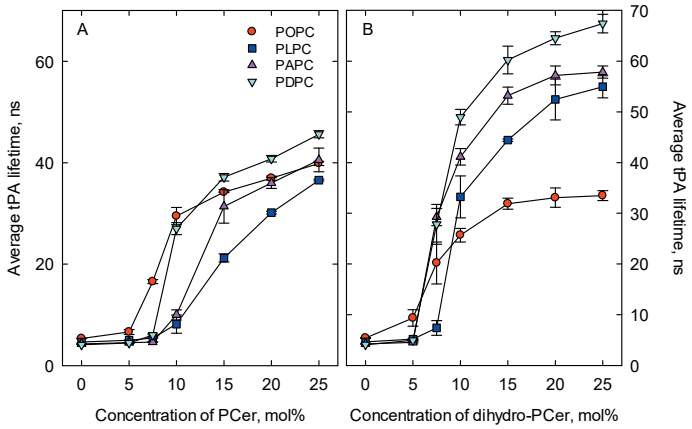

Figure 19. *Average tPA fluorescence lifetime in unsaturated PCs bilayers containing increasing concentrations of Pcer (A) or dihydro-Pcer (B). The experiment was carried out at 23 C with 1 mol% tPA. Each value is the mean ± SEM for n=3. The figure is adapted from paper III with the permission of American Chemical Society.*

The results from our tPA lifetime analysis displayed that the intensity weighted average lifetime of tPA started to increase above 5 mol% of Pcer (Fig. 19A), an indication of Pcer lateral phase segregation in POPC bilayers. This is in good agreement with the previous studies where Pcer was reported to form ordered domains in POPC bilayers at a very low concentration,

around 3-5 mol% (Silva et al., 2006; Ekman et al., 2015; Castro et al., 2007). When we replaced POPC with PLPC, a higher Pcer concentration was needed for the lateral segregation of Pcer in the bilayers (Fig. 19A). There was almost 5 mol% of concentration shift observed for Pcer segregation in PLPC. When additional double bonds were introduced in the sn-2 position of the PCs, as was the case for the PCs containing 20:4 (PAPC) or 22:6 (PDPC), lateral segregation occurred at lower Pcer concentration that was close to the concentrations needed for Pcer in the POPC bilayers. However, slightly higher lateral packing of Pcer-rich phase was observed in PDPC bilayers, as indicated by the tPA fluorescence longest lifetime component (Fig. 20A).

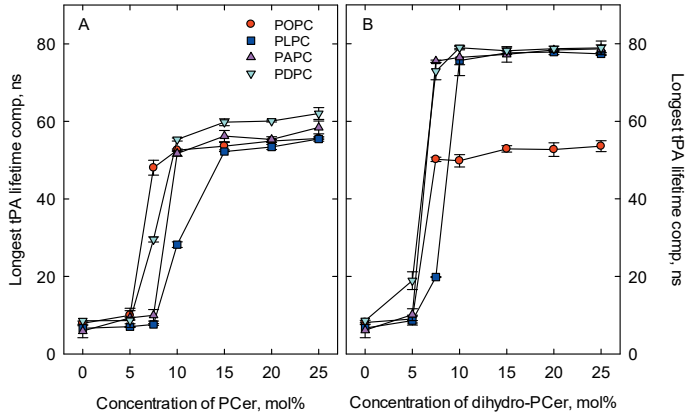

Figure 20. *Longest lifetime component of tPA fluorescence in unsaturated PCs bilayers with increasing concentrations of Pcer (A) or dihydro-Pcer (B). The experiment was carried out at 23 C with 1 mol% tPA. Each value is the mean ± SEM for n=3. The figure is adapted from paper III with the permission of American Chemical Society.*

When we compared the lateral segregation of fully saturated dihydro-Pcer with Pcer in the POPC bilayers, we also observed ceramide-rich phase formation by dihydro-Pcer in the bilayers (Fig. 19B and Fig. 20B). In the PLPC bilayers, the ceramide-rich ordered phase formation by dihydro-Pcer occurred with a slightly higher ceramide concentration compared to other PC bilayers; a similar behavior was also observed for Pcer. The packing properties of ceramide-rich phase formation in POPC bilayers by both Pcer and dihydro-Pcer ware almost identical as observed from the longest tPA life time (Fig. 20 A and B). In the case of PAPC and PDPC bilayers, a significant increase in the order of the dihydro-Pcer-rich phase formation was observed (Fig. 19B and Fig. 20B). The higher longest lifetime component of tPA fluorescence indicated that the ceramide-rich phase formation by dihydro-

Pcer was significantly more ordered than the phase formation with Pcer, with the exception in POPC bilayers (Fig. 20, A and B).

5.3.2 Thermostability of ceramide gel phases in unsaturated PC bilayers

We also performed a temperature-dependent tPA anisotropy approach to study the thermostability and end point of the gel phase melting of Pcer and dihydro-Pcer in PXPC bilayers at a 1:9 molar ratio (Fig. 21). We observed that the Pcer gel phase formation in POPC bilayers showed more thermostability compared to gel phases formed in other PCs.

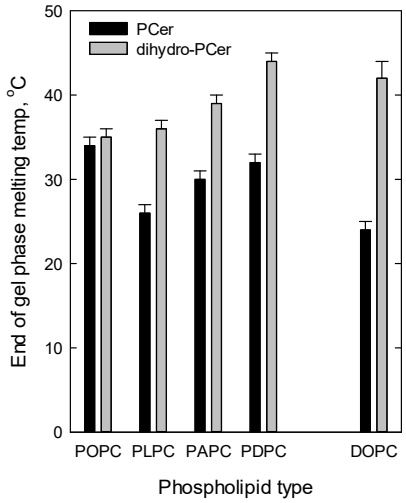

Figure 21. *The end of the gel melting temperature of Pcer or dihydro-Pcer in unsaturated PC bilayers. The compositions were 1:9 mole ratio of ceramides to PC. Each value is the mean ± SEM for n=3. The figure is adapted from paper III with the permission of American Chemical Society.*

The end point of Pcer gel phase melting in POPC was observed at ~34°C, while the lowest gel phase thermostability was observed in PLPC bilayers (~26°C). However, the Pcer gel phase increased in PAPC and PDPC bilayers with the increase of *cis*-double bonds and chain length in the PCs compared to the thermostability observed in the PLPC bilayers. With incorporation of dihydro-Pcer in the PXPC bilayers (at 1:9 ratio), the ceramide-rich gel phase displayed more thermostability compared to the Pcer-rich gel phase formed in the same PC bilayers. Interestingly, dihydro-Pcer-rich gel phase formation in the PXPC bilayers became more thermostable with the increasing unsaturation and chain length of the PCs, which displayed the end point of

the gel phase melting at ~ 35.1°C in the POPC bilayers and up to ~ 44 °C in the PDPC bilayers. We also included DOPC as a dimonounsaturated PC to compare it with POPC. Our results showed that the Pcer-rich gel phase formation in the POPC bilayer was more thermostable compared to the Pcer-rich gel phase formed in the DOPC bilayer. However, the gel phase formation by dihydro-Pcer in the DOPC bilayers was much more stable than in the POPC bilayers, as observed from the much higher end-point temperatures of gel melting ~ 42 °C in DOPC and ~ 35°C in POPC bilayers. Our results indicated that the ceramide-rich phases became more thermostable when more unsaturated PCs were introduced into the mixed bilayers.

We showed how the properties of ceramides are affected in bilayers with increasing level of glycerophospholipid unsaturation. In our study, we have included Pcer because it is one of the most important ceramide species in biological cells. We have also included dihydro-Pcer since it is a structural analog of Pcer that lacks *trans* 4 double bond in the long-chain base. It has been previously reported that the dynamic mobility and intermolecular hydrogen bonding involving the 3-OH can be affected for the absence of the *trans* double bond (Li et al., 2002).

When we compared the properties of ceramides in POPC and DOPC bilayers, we observed that the Pcer gel phase formation was stabilized by sn-1 palmitoyl residue in the POPC and by sn-1 oleoyl residue in DOPC. Because POPC is a hybrid lipid, the saturated chain of POPC may interact with other saturated acyl chains of colipids in the bilayers, whereas its unsaturated chain may not provide favorable interactions with saturated acyl chains (Heberle et al., 2013; Litman et al., 1991). Perhaps this hybrid nature of POPC provides Pcer for more stable gel phase formation in POPC bilayers over the diunsaturated DOPC. We observed the evidence that the end point of the gel phase melting temperature of Pcer shows higher thermostability in POPC bilayers than in DOPC bilayers (Fig. 21). The dihydro-Pcer showed slightly different properties compared to Pcer in the POPC and DOPC bilayers. Significantly, a more stable dihydro-Pcer gel phase formation was observed compared to Pcer gel phase formation in DOPC bilayers. Perhaps the stronger intermolecular hydrogen bonding among dihydro-Pcer molecules could have led to its lower miscibility in these PC bilayers. We have observed the similar behavior for palmitoyl SM and its dihydro analogs (Paper IV).

Pcer and dihydro-Pcer also showed slightly different behavior in the bilayers with increasing unsaturated PCs. The gel phase order and thermostability of

the dihydro-Pcer gel phase increased when the degree of PC unsaturation increased. However, the Pcer gel phase showed higher thermostability in POPC bilayers than in other unsaturated PCs (PLPC, PAPC, and PDPC). The removal of the *trans* double bond in dihydro-Pcer changed the dynamics of the 3-OH and consequently, altered the hydrogen-bonding properties to facilitate dihydro-Pcer lateral segregation. It has been reported that the hydrogen bonding has a significant effect on lateral segregation of ceramides in POPC bilayers (Ekman et al., 2015).

The sn-2 chain length for POPC and PLPC are shorter than for PAPC and PDPC. Thus, in addition to the degree of unsaturation, some of the effects observed in unsaturated PCs bilayer may come from the differences in chain length of the PCs. However, the interactions between the ceramides and PCs were complex. We think these interactions overall were influenced by (i) hydrogen bonding capacity, mostly bonding between ceramides, and also between ceramides and PCs, and by (ii) acyl chain interactions that were influenced by the length and number of the *cis*-double bond in PCs.

5.4 Effect of hydrogen bonding on sphingomyelin/colipid interactions

To study the influence of hydrogen bonding on sphingomyelin (SM) and colipid interactions in fluid bilayers, we included oleoyl or palmitoyl SM and dihydro-SMs, because they differ in their hydrogen bonding properties. We performed a comparative study to investigate the properties of oleoyl or palmitoyl SM with comparable dihydro-SMs. We also investigated how the differences in SM/dihydro-SM hydrogen bonding may influence interactions with cholesterol and ceramides. In our experiments, we carefully controlled the acyl chain order because it can markedly affect the affinity of cholesterol for phospholipid bilayers (Halling 2008). We compared the phospholipid acyl chain order using CTL and DPH anisotropy measurements and also measured the average tPA lifetimes in binary POPC/PSM or POPC/dihydro-PSM. The difference in acyl chain order between pure OSM and dihydro-OSM bilayers was ascertained from DPH anisotropy measurement (Fig. 22), where the dihydro species were more ordered at a given temperature compared to the nondihydro SM. OSM, dihydro-OSM, and POPC bilayers showed similar acyl chain order at 24°C, 28 °C, and 16°C, respectively (Fig. 23, B and C).

Under these experimental conditions, we measured CTL partitioning in the OSM and dihydro-OSM and POPC bilayers.

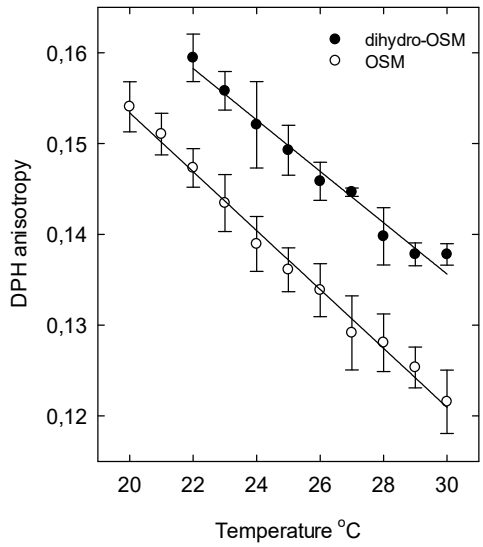

***Figure* 22.** *Bilayer acyl chain order measured from DPH anisotropy. Multilamellar vesicles prepared from pure OSM or pure dhOSM contained 1 mol% DPH. The steady-state anisotropy of DPH was measured as a temperature function (data shown for the 20-30°C temperature interval). Each value is the average ± SD from n = 3–5. The figure is adapted from paper IV with the permission of Elsevier.*

5.4.1 CTL partitioning between the LUVs and CyD

The equilibrium partitioning of CTL between LUVs were prepared from POPC, OSM, or dihydro-OSM and CyD. The interactions between CTL and phospholipids are similar to cholesterol, though CTL is to some extent more polar than cholesterol (Scheidt et al., 2003). It has been reported that the absolute bilayer affinity of CTL is ~5–7 times less than that of cholesterol, though the relative differences in their affinity for SM and PC bilayers are similar (Nystrom et al., 2010). Our results showed that the K_x (partitioning coefficient, mM) of CTL was significantly higher in the dihydro-OSM bilayers (a K_x of ~ 37) compared to the OSM and POPC bilayers (Fig. 23A).

Under the same conditions, similar anisotropy values for CTL and DPH in the bilayers (Fig. 23B and Fig. 23C) further confirmed the identical acyl chain order of the bilayers. The difference in the K_x of the POPC and OSM/dihydro-

OSM bilayers might come from the hydrogen bond stabilization in the OSM/dihydro-OSM bilayers, which is absent in the POPC bilayers. The binary mixtures containing POPC (80 mol %) and either PSM or dihydro-PSM (at 20 mol %) showed that the K_x for CTL was significantly higher ($p < 0.05$) in the POPC/dihydro-PSM bilayers (a K_x of ~ 17.5) compared to the POPC/PSM bilayers (a Kx of ~ 13.5; Fig. 23D). At a similar experimental condition (37°C), we also confirmed the identical acyl chain order of these bilayers; the CTL anisotropy values did not show much difference between the bilayers (Fig. 23E). This was further confirmed by the similar tPA average lifetime values in POPC/PSM and POPC/dihydro-PSM mixtures at 37°C (Fig. 23F).

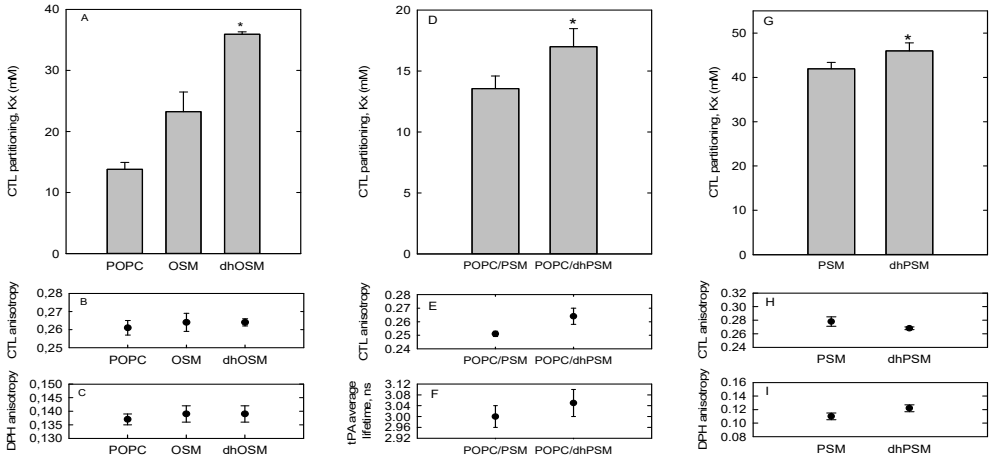

Figure 23. *CTL equilibrium partitioning between the LUVs and CyD. The LUVs (200 nm in diameter) were prepared from either pure POPC, OSM, or dihydro-OSM (A–C); POPC/PSM or POPC/dihydro-PSM (4:1 molar ratio; D–F); or pure PSM or dihydro-PSM (G–I), and they contained 2 mol% CTL at the start of the experiment. The K_x for CTL partitioning was determined at 16°C (POPC), 24°C (OSM), 28°C (dihydro-OSM), 37°C (POPC/PSM and POPC/dihydro-PSM), 50°C (PSM), or 53.5°C (dihydro-PSM) to achieve close to equal acyl chain order in the respective bilayers. Panels A, D, and G show the K_x values for each type of LUV, and panels B, E, and H show the measured CTL anisotropy values at the start of the experiment. Finally, panels C and I show the DPH anisotropy values at the start of the experiment, and panel F shows the average lifetime component of tPA. The asterisk indicates a statistically significant difference between the compared SM bilayers in each panel ($P < 0.001$ for A, $P < 0.05$ for D, G). The difference between CTL partitioning to POPC and the SM bilayers shown in panel A was also significant ($P < 0.001$). The value pairs in panels B, E, and H and in C, F, and I were not significantly different ($P > 0.05$). Each value is the average $\pm$ SD from n=3–5. Note that dihydro is indicated with dh. The figure is adapted from paper IV with the permission of Elsevier.*

Since DPH partitioning into ordered and disordered phases are similar (Kaiser and London, 1998), DPH anisotropy in detecting the acyl chain order in the SM-rich phase would not provide a reliable prediction. Therefore, fluorescence lifetime analysis of tPA was performed to detect the acyl chain order of the more ordered SM-rich phase (Nyholm et al., 2011). In pure PSM and dihydro-PSM bilayers, the K_x of CTL showed significantly higher values ($p < 0.05$) in the dihydro-PSM bilayers (a $K_x \sim 46.5$) compared to that of the PSM bilayers (a $K_x \sim 42$; see Fig. 23G).

5.4.2 Cholesterol-induced ordering of the OSM and dihydro-OSM bilayers

We studied the interactions of cholesterol with OSM and dihydro-OSM and investigated the cholesterol-induced ordering effect on these bilayers. Cholesterol was added in the bilayers with small increments (between 3–21 mol %), and the bilayer phase behavior was detected using tPA fluorescence lifetime analysis.

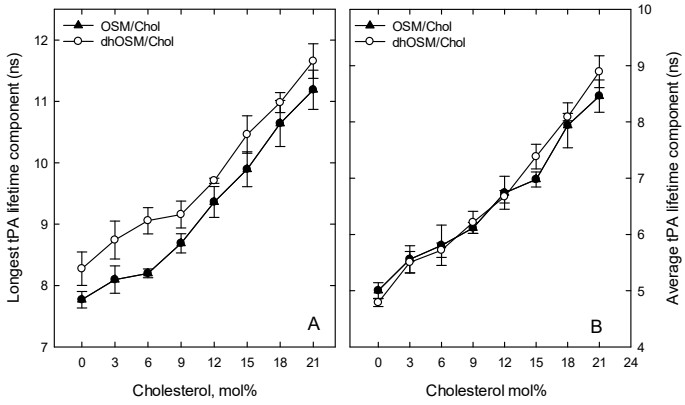

Figure 24. *Cholesterol-induced ordering of the OSM and dihydro-OSM bilayers. MLVs containing OSM or dihydro-OSM and increasing amounts of cholesterol and 1 mol% tPA were prepared. A fluorescence lifetime analysis of tPA emission was performed at 24°C for the OSM bilayers (filled triangles) and 28°C for the dihydro-OSM bilayers (open circles). Panel A shows the longest lifetime of tPA, and panel B shows the average lifetime of tPA as a function of the cholesterol concentration. Each value is the average ± SD from n=3–5. Note that dihydro is indicated with dh. The figure is adapted from paper IV with the permission of Elsevier.*

Results from our lifetime analysis showed that with the increment of cholesterol in the bilayers, both the average and longest lifetime component of tPA fluorescence increased almost linearly. Because tPA fluorescence tends to show a higher affinity for ordered phase, the increase in the lifetime of tPA

was clearly indicative of an increased ordered environment. At identical cholesterol concentrations, the longest fluorescence lifetime component of tPA was slightly longer in the dihydro-OSM bilayers compared to that in the OSM bilayers (Fig. 24A), though the tPA average lifetime was almost similar in both bilayers (Fig. 24B). In general, the average fluorescence lifetime of tPA included contributions from all phases present, while the longest lifetime component was associated with tPA localized in the most ordered environment. Similar values for tPA average lifetime in both the OSM and dihydro-OSM bilayers indicated that the fractional contribution from the more ordered cholesterol-rich phase was small. In OSM/dihydro-OSM bilayers, the lifetime of tPA was comparatively shorter than was reported in a liquid-ordered phase composed of saturated SM and cholesterol (Nyholm et al., 2011). Slightly longer lifetime in dihydro-OSM bilayers, as observed from the longest lifetime component of tPA, indicates that cholesterol induced a more ordered phase in the dihydro-OSM bilayers compared to that in OSM bilayers.

5.4.3 Ceramide and diacylglycerol segregation in OSM and dihydro-OSM bilayers

Ceramides or DPG-induced ordered phase formation in fluid OSM or dihydro-OSM bilayers were investigated using time-resolved analysis of tPA fluorescence. It has been observed that in fluid POPC bilayers, Pcer can induce ordered phase formation at lower concentrations, above 3–4 mol% ceramides (Silva et al., 2006). In the same POPC bilayers, a chain match diacylglycerol was observed to segregate; however, a higher concentration was needed for phase segregation by diacylglycerol compared to ceramides (Ekman et al., 2015).

The ceramide-ordered phase has greater stability due to the hydrogen bonding efficiency among the ceramides (Ekman et al., 2015). In our experiment, we selected the initial condition such that the acyl chain order of the bilayers was equal for both OSM and dihydro-OSM. In the OSM bilayers, Pcer-20:1 formed an ordered phase at concentrations above 6 mol%, whereas no ordered phase formation was observed by DPG in the same bilayers (Fig. 25A). Interestingly, in the dihydro-OSM bilayers, both Pcer-20:1 and DPG more readily formed an ordered phase than in the OSM bilayer. Pcer-20:1 started to form an ordered phase in the dihydro-OSM bilayers, even at a lower concentration (> 2 mol %). Thus, Pcer-20:1 and DPG tended to show a

difference in ordered phase formation in the bilayers, which supports the idea that hydrogen bonding stabilized the self-association of ceramides. Moreover, differences in the hydrogen bonding of the OSM and dihydro-OSM bilayers also influenced the phase formation of Pcer-20:1 and DPG; the self-association of these lipids was better in the dihydro-OSM bilayers than in the OSM bilayers.

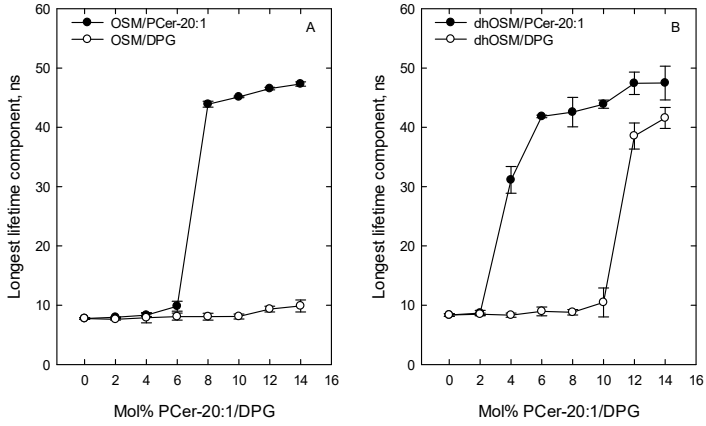

Figure 25. *Formation of a gel phase by Pcer-20:1 and DPG in the OSM and dihydro-OSM bilayers. MLVs with the indicated lipid compositions were prepared together with 1 mol% tPA. As a function of added Pcer-20:1 (filled symbols) or DPG (open symbols), the longest tPA lifetime, indicative of the formation of a gel phase, of each sample was determined at 24°C (OSM; A) or 28°C (dihydro-OSM; B). At these temperatures, the acyl chain order of the pure OSM and pure dihydro-OSM bilayers were initially similar. Each value is the average ± SD from n=3–5. Note that dihydro is indicated with dh. The figure is adapted from paper IV with the permission of Elsevier.*

To investigate the effect of hydrogen bonding on SM/colipid interactions, we have used SM and its chain-matched dihydro-SM which are significantly different in hydrogen bonding properties (Talbott et al., 2000; Ferguson-Yankey et al., 2000; Kinoshita et al., 2014). The effect of hydrogen bonding on phospholipid/cholesterol interactions has been reported previously in bilayer membranes (Lonnfors et al., 2011). It has been observed that phospholipid/cholesterol interactions are also influenced by the length of phospholipid acyl chain (Jaikishan and Slotte, 2011), degree of unsaturation (Engberg et al., 2016), acyl chain order (Halling et al., 2008), and effects due to the phospholipid headgroup (Bjorkbom et al., 2010; Huang et al., 1999b; 1999c). The equilibrium partitioning of CTL was performed to measure the

sterol affinity of the unilamellar bilayers. We carefully controlled the similar bilayer acyl chain order of SM and dihydro-SM by varying the experimental temperature. Our results demonstrated that the bilayer affinity of CTL/cholesterol was higher with dihydro-SM than with SM bilayers. It was also noticed that the sterol showed a higher affinity for SM bilayers than for comparable PC bilayers (Fig. 23A, this study, and Fig. 1 in Halling 2008). We think that the difference in hydrogen bonding properties of the two types of SMs causes higher sterol affinity for the dihydro-SM bilayers compared to the matched SM bilayers.

We also detected the presence of the cholesterol-rich phase in the OSM or dihydro-OSM bilayers using tPA fluorescence lifetime analysis. Our results suggested that the cholesterol-enriched phase was slightly more ordered in dihydro-OSM bilayers compared to OSM bilayers, as a higher longest lifetime component was observed in dihydro-OSM bilayers (Fig. 24). Thus, our finding suggest a more favorable and closer interaction between cholesterol and dihydro-OSM. We think this interaction is partially resulted from the hydrogen bonding properties of dihydro-OSM, which are different from those of OSM. It has been observed that the hydrogen-bonding properties of ceramides and cholesterol are different, even though both are amphiphilic molecules having small polar functions at their water interface. Ceramides contain two hydrogen bond-donating hydroxyl groups on C1 and C3, whereas cholesterol has only one hydroxyl in the C3-position. Moreover, ceramide acyl chains are amide-linked and this functional group plays a major role in hydrogen-bonding properties of ceramides. It has also been reported that cholesterol and ceramide show different affinity to the headgroup properties of their interacting partner molecules (Bjorkbom et al., 2010; Artetxe et al., 2013). In addition to favorable van derWaals interactions, the hydrogen bonding efficiency of ceramides promotes favorable stabilization of ceramide/SM interaction over SM/cholesterol interaction. When a comparative study was performed to detect the ordered phase formation by Pcer-20:1 and DPG in the dihydro-OSM and OSM bilayers using tPA lifetime analysis, we observed that DPG required much higher bilayer concentration to form an ordered phase. Our findings are in agreement with the report on the lateral segregation of Pcer-20:1 and DPG in POPC bilayers (Ekman et al., 2015). It indicates that the differences in hydrogen-bonding properties between ceramides and matched diglycerides significantly influence their interactions and lateral segregation in the bilayers.

It has been reported that compared to *cis* double bonds, *trans* double bonds at the same position provide better hydrogen bonding efficiency among SMs (Janosi and Gorfe, 2010). However, in hydrogen bond formation the double bond itself is not a partner, therefore it causes an indirect effect by altering the packing properties or hydrogen bonding.

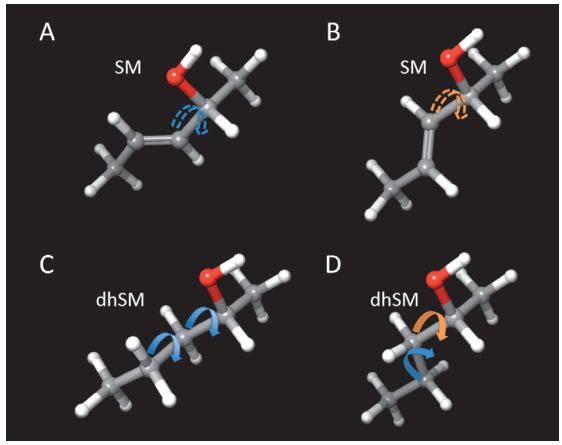

Figure 26. *Energy-minimized molecular structures of a partial SM and dihydro-SM fragment. Structures A and B represent SM, and fragments C and D depict dihydro-SM. The blue dotted arrow (A) indicates the restricted rotation of the C-C bond. The blue complete arrow (C and D) indicates less hindered rotation of the C-C bond. The orange dotted arrow (B) indicates the different orientation of the bond in B compared to A, but its rotation is still hindered. The complete orange arrow in D indicates the changed orientation compared to in C, with the rotation of the C-C bond less hindered. The energy difference between configuration A and B is only about 0.21 kcal/mol, which means that both configurations are likely. The figure is adapted from paper IV with the permission of Elsevier.*

As observed from the quantum chemical calculations, the rotational freedom of the neighboring C-C bond was restricted due to the presence of *trans* double bond on the sphingoid base of SM. Two possible likely conformations are presented in Fig. 26, A and B. The conformation presented in Fig. 26A is favored over that showed in Fig. 26B, the energy difference between these two conformations was only ~ 0.21 kcal/mol. Due to the absence of *trans* double bond in dihydro-SM, no restriction in rotational freedom was reported for this molecule. In the case of dihydro-SM rather an increased rotational freedom of 3-OH was observed (Fig. 26, C and D). Because hydrogen bonds are directional, a more flexible 3-OH in dihydro-SM may provide better hydrogen-bonding efficiency in this molecule than in SM, where 3-OH is restricted.

6. CONCLUSIONS

Because ceramides significantly affect cellular events, e.g., apoptosis, cell sensing, and necrosis and also contribute as membrane structural components, studying their properties and behavior in membranes is highly important. In this thesis, we have systematically investigated how the structural variation in ceramides can influence their molecular properties and their interactions with other lipids that are present in the bilayers. We have also examined how the structure of the associated lipids can influence the ceramide-rich phases in bilayer membranes. Important conclusions drawn from our studies are presented here.

In papers I–II, we demonstrated how specific structural variations in ceramides concerning the length of both *N*-acyl chains and long-chain base, interfacial hydroxylation, identity of the headgroup, and the position of *cis*-double bonds in the chains can influence their membrane bilayer properties. Based on the results of Paper I and II, our observations are the following:

i. The length of the long-chain base of ceramides has a major effect on ceramide-colipid interactions compared to the effect of *N*-linked acyl chain length.
ii. Ceramide-colipid interactions are asymmetric. We think this asymmetric nature of ceramide-colipid interactions could be explained by the asymmetric location of the functional groups involved in hydrogen bonding.
iii. The consequences of interfacial hydroxylation and the *N*-acyl chain length of ceramides, cause relatively small variation on their bilayer properties.
iv. The presence of *cis*-double bonds and their comparative position in the ceramide acyl chains, cause major effect on the properties of ceramides compared to common saturated and hydroxylated ceramide species.

In paper III, we examined the interactions of saturated ceramides in unsaturated glycerophospholipid bilayers and demonstrated how the properties of ceramides are influenced by the degree of unsaturation of different glycerophospholipids. A clear effect was observed on dihydro-Pcer properties with the increased unsaturation of the sn-2 acyl chains of the PCs. These interactions between ceramides and PCs were affected both by the *trans*-4 double bond of Pcer by the palmitoyl acyl in the sn-1 position and by the overall degree of unsaturation of the sn-2 acyl chain of the PCs. Our

findings could be important in studying the behavior of ceramide or dihydroceramide in membranes of endoplasmic reticulum, since this is the site for biosynthesis of these ceramides and also these membranes are thought to be abundant in unsaturated glycerophospholipids.

In paper IV, we explored how the interactions between sphingomyelin (SM) and colipids (ceramides and cholesterol) can be affected by hydrogen-bonding properties. However, it is also obvious that in hydrated bilayers other types of interactions (hydrophobic or van der Waals interactions, steric effects, headgroup effects, etc.) are similarly important for lipid interactions. We used sphingomyelins (OSM and dihydro-OSM) with different hydrogen-bonding capacities and observed significant consequences of their interactions with ceramides and cholesterol. Our findings demonstrated that hydrogen bonding is important for sterol/SM and ceramide/SM interactions, and these interactions are distinctly affected by hydrogen bonding.

Our results demonstrated that specific small structural variation may lead to differences in behavior of ceramides, which could have possible consequences in distinct cell or tissue types. Some of these effects could be more dramatic, whereas others could cause only fine adjustment in interaction of ceramides with other lipids in the membrane. In mammalian ceramides, the variations in the acyl chain lengths are more common than the variation in long-chain base lengths. Therefore, we think that the unique properties of ceramides may come from variable acyl chain lengths that do not have a dramatic impact on gel-phase properties of ceramides. For the substrate properties of ceramides in synthesis of more complex sphingolipids and for their specific interactions with membrane proteins, these unique properties of ceramides could be pivotal.

Overall, we have reported how the biophysical properties of ceramides are influenced by their molecular structure and the colipids present in the membrane bilayers, which may have distinct effects on cell physiology. Our results were obtained from model membrane studies, however it partially characterize the lipid interactions of more complex biological membranes. In future, it will be interesting to introduce different ceramide species into cells and to study how their properties and interactions with colipids may influence such complex system.

REFERENCES

Adam, D., M. Heinrich, D. Kabelitz, and S. Schutze. 2002. Ceramide: does it matter for T cells? *Trends in Immunology.* 23: 1-4.

Airola, M. V., and Y. A. Hannun. 2013. Sphingolipid metabolism and neutral sphingomyelinases. *Handb Exp Pharmacol.* 215: 57-76.

Alanko, S. M., K. K. Halling, S. Maunula, J. P. Slotte, and B. Ramstedt. 2005. Displacement of sterols from sterol/sphingomyelin domains in fluid bilayer membranes by competing molecules. *Biochim. Biophys. Acta.* 1715: 111-121.

Ali, M. R., K. H. Cheng, and J. Huang. 2006. Ceramide drives cholesterol out of the ordered lipid bilayer phase into the crystal phase in 1-palmitoyl-2-oleoyl-sn-glycero-3-phosphocholine/cholesterol/ceramide ternary mixtures. *Biochemistry.* 45: 12629-12638.

Anliker, B., and J. Chun. 2004. Lysophospholipid G protein-coupled receptors. *J Biol Chem.* 279: 20555-20558.

Artetxe, I., C. Sergelius, M. Kurita, S. Yamaguchi, S. Katsumura, J. P. Slotte, and T. Maula. 2013. Effects of sphingomyelin headgroup size on interactions with ceramide. *Biophys. J.* 104: 604-612.

Babiychuk, E. B., K. Monastyrskaya, S. Potez, and A. Draeger. 2009. Intracellular Ca^{2+} operates a switch between repair and lysis of streptolysin O-perforated cells. *Cell Death. Differ.* 16: 1126-1134.

Bangham, A. D., and R. W. Horne. 1964. Negative staining of phospholipids and their structural modification by surface-active agents as observed in the electron microscope. *J. Mol. Biol.* 8: 660-668.

Bangham, A. D., M. M. Standish, and J. C. Watkins. 1965. Diffusion of univalent ions across the lamellae of swollen phospholipids. *J. Mol. Biol.* 13: 238-252.

Barbosa-Barros, L., A. De la Maza, P. Walther, J. Estelrich, and O. Lopez. 2008. Morphological effects of ceramide on DMPC/DHPC bicelles. *J Microscopy.* 230: 16-26.

Barenholz, Y. 1984. *Physiology of Membrane Fluidity* (Shinitzky, M., Ed.). 1: 131-174, CRC Press, Boca Raton, FL.

Barenholz, Y., and T. E. Thompson. 1980. Sphingomyelins in bilayers and biological membranes. *Biochim. Biophys. Acta.* 604: 129-158.

Barenholz, Y., and T. E. Thompson. 1999. Sphingomyelin: biophysical aspects. *Chem. Phys. Lipids.* 102: 29-34.

Bartke N., and Y. A. Hannun. 2009. Bioactive sphingolipids: metabolism and function. *J. Lipid Res.* 50: S91-96.

Bjorkbom, A., T. Rog, K. Kaszuba, M. Kurita, S. Yamaguchi, M. Lönnfors, T. K. M. Nyholm, I. Vattulainen, S. Katsumura, and J. P. Slotte. 2010. Effect of sphingomyelin headgroup size on molecular properties and interactions with cholesterol. *Biophys. J.* 99: 3300-3308.

Bjorkqvist, Y. J., T. K. Nyholm, J. P. Slotte, and B. Ramstedt. 2005. Domain formation and stability in complex lipid bilayers as reported by cholestatrienol. *Biophys. J.* 88: 4054-4063.

Boggs, J. M. 1980. Intermolecular hydrogen bonding between lipids: influence on organization and function of lipids in membranes. *Can. J. Biochem*. 10: 755-770.

Bonosi, F., G. Gabrieklli, E. Margheri, and G. Martini. 1990. Effect of the addition of ceramide to dioleoylphosphatidylcholine vesicles: an ESR and SEM study. *Langmuir*. 6: 1769-1773.

Boulgaropoulos, B., Z. Arsov, P. Laggner, and G. Pabst. 2011. Stable and unstable lipid domains in ceramide-containing membranes. *Biophys. J.* 100: 2160-2168.

Brocklyn, J. R., M. H. Graler, G. Bernhardt, J. P. Hobson, M. Lipp, and S. Spiegel. 2000. Sphingosine-1-phosphate is a ligand for the G protein-coupled receptor EDG-6. *BLOOD*. 95: 2624-2629.

Brockman, H. L., M. M. Momsen, R. E. Brown, L. He, J. Chun, H. S. Byun, and R. Bittman. 2004. The 4,5-double bond of ceramide regulates its dipole potential, elastic properties, and packing behavior. *Biophys. J.* 87: 1722-1731.

Brown, D.A., and E. London. 2000. Structure and Function of Sphingolipid- and Cholesterol-rich Membrane Rafts. *J. Biol. Chem*. 275: 17221-17224.

Brumm, T., K. Jorgensen, O. G. Mouritsen, and T. M. Bayerl. 1996. The effect of increasing membrane curvature on the phase transition and mixing behavior of a dimyristoyl-sn-glycero-3-phosphatidylcholine/distearoyl-sn-glycero-3-phosphatidylcholine lipid mixture as studied by Fourier transform infrared spectroscopy and differential scanning calorimetry. *Biophys. J.* 70: 1373-1379.

Brzustowicz, M. R.; V. Cherezov, M. Caffrey, W. Stillwell, and S. R. Wassall. 2002. Molecular organization of cholesterol in polyunsaturated membranes: microdomain formation. *Biophys. J.* 82: 285-298.

Busto, J. V., A. B. Garcı´a-Arribas, J. Sot, A. Torrecillas, J. C. Go´mez-Ferna´ndez, F. M. Goni, and A. Alonso. 2014. Lamellar gel (lb) phases of ternary lipid composition containing ceramide and cholesterol. *Biophys. J.* 106: 621-630.

Busto, J. V., J. Sot, J. Requejo-Isidro, F. M. Goni, and A. Alonso. 2010. Cholesterol displaces palmitoylceramide from its tight packing with palmitoylsphingomyelin in the absence of a liquiddisordered phase. *Biophys. J.* 99: 1119-1128.

Busto, J. V., M. L. Fanani, L. De Tullio, J. Sot, B. Maggio, F. M. Goni, and A. Alonso. 2009. Coexistence of immiscible mixtures of palmitoylsphingomyelin and palmitoylceramide in monolayers and bilayers. *Biophys. J.* 97: 2717-2726.

Calhoun, W. I., and G. G. Shipley. 1979. Fatty acid composition and thermal behavior of natural sphingomyelins. *Biochim. Biophys. Acta*. 555: 435-441.

Cantor, R. S. 1997. Lateral Pressures in Cell Membranes: A Mechanism for Modulation of Protein Function. *J. Phys. Chem*. 10: 1723-1725.

Carpinteiro, A., C. Dumitru, M. Schenck, and E. Gulbins. 2008. Ceramide-induced cell death in malignant cells. *Cancer Lett.* 264: 1-10.

Carrer, D. C., and B. Maggio. 1999. Phase behavior and molecular interactions in mixtures of ceramide with dipalmitoylphosphatidylcholine. *J. Lipid Res.* 40: 1978-1989.

Carter, H. E., F. J. Glick, W. P. Norris, and G. E. Phillips. 1947. Biochemistry of the Sphingolipids. III. Structure of Sphingosine. *J. Biol. Chem.* 170: 285-294.

Castro, B. M., R. F. de Almeida, L. C. Silva, A. Fedorov, and M. Prieto. 2007. Formation of ceramide/sphingomyelin gel domains in the presence of an unsaturated phospholipid: a quantitative multiprobe approach. *Biophys. J.* 93: 1639-1650.

Castro, B. M., L. C. Silva, A. Fedorov, R. F. de Almeida, and M. Prieto. 2009. Cholesterol-rich fluid membranes solubilize ceramide domains: implications for the structure and dynamics of mammalian intracellular and plasma membranes. *J. Biol. Chem.* 284: 22978-22987.

Castro, B. M., M. Prieto, and L. C. Silva. 2014. Ceramide: A simple sphingolipid with unique biophysical properties. *Prog. Lipid Res.* 54: 53-67.

Chakrabarti, R. M., S. A. Ingham, J. Kozlitina, A. Gay, J. C. Cohen, A. Radhakrishnan, and H. H. Hobbs. 2017. Variability of cholesterol accessibility in human red blood cells measured using a bacterial cholesterol-binding toxin. *eLife*. 6: e23355.

Chalfant, C. E., K. Kishikawa, M. C. Mumby, C. Kamibayashi, A. Bielawska, and Y. A. Hannun. 1999. Long chain ceramides activate protein phosphatase-1 and protein phosphatase-2A. Activation is stereospecific and regulated by phosphatidic acid. *J. Biol. Chem*. 274: 20313-20317.

Chalfant, C. E., Z. Szulc, P. Roddy, A. Bielawska, and Y. A. Hannun. 2004. The structural requirements for ceramide activation of serine-threonine protein phosphatases. *J. Lipid Res.* 45: 496-506.

Chan, Y. H., and S. G. Boxer. 2007. Model membrane systems and their applications. *Curr. Opin. Chem. Biol*. 11: 581-587.

Chen, H., R. Mendelsohn, M. E. Rerek, and D. J. Moore. 2000. Fourier transform infrared spectroscopy and differential scanning calorimetry studies of fatty acid homogeneous ceramide 2. *Biochim. Biophys. Acta.* 1468: 293-303.

De Almeida, R. F., A. Fedorov, and M. Prieto. 2003. Sphingomyelin/phosphatidylcholine/cholesterol phase diagram: boundaries and composition of lipid rafts. *Biophys. J.* 85: 2406-2416.

De Vries, A. H., S. Yefimov, A. E. Mark, and S. J. Marrink. 2005. Molecular structure of the lecithin ripple phase. *Proc. Natl. Acad. Sci. U. S. A.* 102: 5392-5396.

Dobrowsky, R. T., C. Kamibayashili, M. C. Mumbyli, and Y. A. Hannun. 1993. Ceramide Activates Heterotrimeric Protein Phosphatase 2A. *J. Biol. Chem*. 268: 15523-15530.

Dougherty, R. M., C. Galli, A. Ferro-Luzzi, and J. M. Iacono. 1987. Lipid and phospholipid fatty acid composition of plasma, red blood cells, and platelets and how they are affected by dietary lipids: a study of normal subjects from Italy, Finland, and the USA. *Am. J. Clin. Nutr*. 45: 443-455.

Dreschers, S., P. Franz, C. A. Dumitru, B. Wilker, K. Jahnke, and E. Gulbins. 2007. Infections with human rhinovirus induce the formation of distinct functional membrane domains. *Cell Physiol. Biochem*. 20: 241-254.

Dupuy, F. G., and B. Maggio. 2014. N-acyl chain in ceramide and sphingomyelin determines their mixing behavior, phase state, and surface topography in Langmuir films. *J. Phys. Chem. B.* 118: 7475-7487.

Ekholm, O., S. Jaikishan, J. P. Slotte. 2011. Membrane bilayer properties of sphingomyelins with amide-linked 2- or 3-hydroxylated fatty acids. *Biochim. Biophys. Acta*. 1808: 727-732.

Ekman, P., T. Maula, S. Yamaguchi, T. Yamamoto, T. K. M. Nyholm, S. Katsumura, and J. P. Slotte. 2015. Formation of an ordered phase by ceramides and diacylglycerols in a fluid phosphatidylcholine bilayer - correlation with structure and hydrogen bonding capacity. *Biochim. Biophys. Acta*. 1848: 2111-2117.

Engberg, O., V. Hautala, T. Yasuda, H. Dehio, M. Murata, J. P. Slotte, T. K. M. Nyholm. 2016. The Affinity of Cholesterol for Different Phospholipids Affects Lateral Segregation in Bilayers. *Biophys. J*. 111(3):546-556.

Eyster, K. M. 2007. The membrane and lipids as integral participants in signal transduction: lipid signal transduction for the non-lipid biochemist. *Adv. Physiol Educ*. 31: 5-16.

Fahy, E., S. Subramaniam, H. A. Brown, C. K. Glass, A. H. Merrill, Jr., R. C. Murphy, C. R. Raetz, D. W. Russell, Y. Seyama, W. Shaw, T. Shimizu, F. Spener, G. van Meer, M. S. VanNieuwenhze, S. H. White, J. L. Witztum, and E. A. Dennis. 2005. A comprehensive classification system for lipids. *J. Lipid Res.* 46: 839-861.

Fanzo, J. C., M. P. Lynch, H. Phee, M. Hyer, A. Cremesti, H. Grassme, J. S. Norris, K. M. Coggeshall, B. R. Rueda, A. B. Pernis, R. Kolesnick, and E. Gulbins. 2003. CD95 rapidly clusters in cells of diverse origins. *Cancer Biol. Ther*. 2: 392-395.

Farwanah, H., B. Pierstorff, C. E. Schmelzer, K. Raith, R. H. Neubert, T. Kolter, and K. Sandhoff. 2007. Separation and mass spectrometric characterization of covalently bound skin ceramides using LC/APCI-MS and Nano-ESI-MS/MS. *J. Chromatogr. B Analyt. Technol. Biomed. Life Sci.* 852: 562-570.

Ferguson-Yankey, S. R., D. Borchman, K. G. Taylor, D. B. DuPré, and M. C. Yappert. 2000. Conformational studies of sphingolipids by NMR spectroscopy. I. Dihydrosphingomyelin. *Biochim. Biophys. Acta*. 1467: 307-325.

Fidorra, M., L. Duelund, C. Leidy, A. C. Simonsen, and L. A. Bagatolli. 2006. Absence of fluidordered/fluid-disordered phase coexistence in ceramide/POPC mixtures containing cholesterol. *Biophys. J.* 90: 4437-4451.

Futerman, A. H. 2002. *Ceramide Signaling*. Kluwer Academic/Plenum Publishers, New York, USA.

Fyrst, H., D. R. Herr, G. L. Harris, and J. D. Saba. 2004. Characterization of free endogenous C14 and C16 sphingoid bases from Drosophila melanogaster. *J. Lipid Res.* 45: 54-62.

García-Barros, M., N. Coant, T. Kawamori, M. Wada, A. J. Snider, J. P. Truman, Wu BX, H. Furuya, C. J. Clarke, A. B. Bialkowska, A. Ghaleb, V. W. Yang, L. M. Obeid, and Y. A. Hannun. 2016. Role of neutral ceramidase in colon cancer. *FASEB J.* 12: 4159-4171.

Goldschmidt-Arzi, M., E. Shimoni, H. Sabanay, A. H. Futerman, and L. Addadi. 2011. Intracellular localization of organized lipid domains of C16-ceramide/cholesterol. *J. Struct. Biol.* 175: 21-30.

Gorter, E., and F. Grendel. 1925. On bimolecular layers of lipoids on the chromocytes of the blood. *J. Exp. Med*. 41: 439-443.

Grassme, H., A. Riehle, B Wilker, and E. Gulbins. 2005. Rhinoviruses Infect Human Epithelial Cells via Ceramide-enriched Membrane Platforms. *J. Biol. Chem*. 280: 26256-26262.

Grassme, H., V. Jendrossek, A. Riehle, G. von Kurthy, J. Berger, H. Schwarz, M. Weller, R. Kolesnick, and E. Gulbins. 2003. Host defense against Pseudomonas aeruginosa requires ceramide-rich membrane rafts. *Nat. Med*. 9: 322-330.

Grösch, S., S. Schiffmann, and G. Geisslinger. 2012. Chain length-specific properties of ceramides. *Prog. Lipid Res*. 51: 50-62.

Gulbins, E. 2003. Regulation of death receptor signaling and apoptosis by ceramide. *Pharmacol. Res*. 47: 393-399.

Gulbins, E., S. Dreschers, B. Wilker, and H. Grassme. 2004. Ceramide, membrane rafts and infections. *J. Mol. Med*. 82: 357-63.

Gulbins, E., and Li PL. 2006. Physiological and pathophysiological aspects of ceramide. *Am. J. Physiol. Regul. Integr. Comp. Physiol*. 290: 11-26.

Halling, K. K., B. Ramstedt, J. H. Nyström, J. P. Slotte, and T. K. Nyholm. 2008. Cholesterol interactions with fluid-phase phospholipids: effect on the lateral organization of the bilayer. *Biophys. J.* 95: 3861-3871.

Hanada, K., K. Kumagai, N. Tomishige, and M. Kawano. 2007. CERT and intracellular trafficking of ceramide. *Biochim. Biophys. Acta.* 1771: 644-653.

Hannun, Y. A. 1996. Functions of ceramide in coordinating cellular responses to stress. *Science.* 274: 1855-1859.

Hannun, Y. A., and C. Luberto. 2000. Ceramide in the eukaryotic stress response. *Trends Cell Biol.* 10: 73-80.

Hannun, Y. A., and L. M. Obeid. 2008. Principles of bioactive lipid signalling: lessons from sphingolipids. *Nat. Rev. Mol. Cell Biol*. 9: 139-150.

Hannun, Y. A., and L. M. Obeid. 2011. Many ceramides. *J. Biol. Chem*. 286: 27855-27862.

Heberle, F. A., M. Doktorova, S. L. Goh, R. F. Standaert, J. Katsaras. and G. W. Feigenson. 2013. Hybrid and nonhybrid lipids exert common effects on membrane raft size and morphology. *J. Am. Chem. Soc*. 135: 14932-14935.

Heimburg, T. 2007. *Thermal biophysics of membranes*. Wiley-VCH Verlag GmbH & Co KGaA, Weinheim, Germany.

Heinrich, M., M. Wickel, W. Schneider-Brachert, C. Sandberg, J. Gahr, R. Schwandner, T. Weber, P. Saftig, C. Peters, J. Brunner, M. Krönke, S. Schütze. 1999. Cathepsin D targeted by acid sphingomyelinasederived ceramide. *EMBO J.* 18: 5252-5263.

Hemminga, M. A., J. C. Sanders, C. J. A. M. Wolfs, and R. B. Spruijt. 1993. A. Watts (Ed.). *Protein–Lipid Interactions, New Comprehensive Biochemistry*, Elsevier, Amsterdam.

Hertz, R., and Y. Barenholz. 1975. Permeability and integrity properties of lecithin-sphingomyelin liposomes. *Chem. Phys. Lipids*. 15: 138-156.

Hill, W. G., and M. L. Zeidel. 2000. Reconstituting the barrier properties of a water-tight epithelial membrane by design of leaflet-specific liposomes. *J. Biol. Chem*. 275: 30176-30185.

Holopainen, J. M., J. Y. Lehtonen, and P. K. Kinnunen. 1997. Lipid microdomains in dimyristoylphosphatidylcholine-ceramide liposomes. *Chem. Phys. Lipids.* 88: 1-13.

Holopainen, J. M., M. Subramanian, and P. K. Kinnunen. 1998. Sphingomyelinase induces lipid microdomain formation in a fluid phosphatidylcholine/sphingomyelin membrane. *Biochemistry.* 37: 17562-17570.

Holopainen, J. M., J. Lemmich, F. Richter, O. G. Mouritsen, G. Rapp, and P. K. Kinnunen. 2000. Dimyristoylphosphatidylcholine/C16:0-ceramide binary liposomes studied by differential scanning calorimetry and wide- and small-angle x-ray scattering. *Biophys. J.* 78: 2459-2469.

Hsueh, Y. W., R. Giles, N. Kitson, and J. Thewalt. 2002. The effect of ceramide on phosphatidylcholine membranes: a deuterium NMR study. *Biophys. J.* 82: 3089-3095.

Huang, H. W., E. M. Goldberg, and R. Zidovetzki. 1996. Ceramide induces structural defects into phosphatidylcholine bilayers and activates phospholipase A2. *Biochem. Biophys. Res. Commun.* 220: 834-838.

Huang, H. W., E. M. Goldberg, and R. Zidovetzki. 1998. Ceramides perturb the structure of phosphatidylcholine bilayers and modulate the activity of phospholipase A2. *Eur. Biophys. J.* 27: 361-366.

Huang, C., and S. Li. 1999a. Calorimetric and molecular mechanics studies of the thermotropic phase behavior of membrane phospholipids. *Biochim. Biophys. Acta.* 1422: 273-307.

Huang, J., and G.W. Feigenson. 1999b. A microscopic interaction model of maximum solubility of cholesterol in lipid bilayers. *Biophys. J.* 76: 2142-2157.

Huang, J., J. T. Buboltz, and G. W. Feigenson. 1999c. Maximum solubility of cholesterol in phosphatidylcholine and phosphatidylethanolamine bilayers. *Biochim. Biophys. Acta.* 1417: 89-100.

Huang, W. C., C. L. Chen, Y. S. Lin, and C. F. Lin. 2011. Apoptotic sphingolipid ceramide in cancer therapy. *J. Lipids.* 2011: 1-15.

Huwiler, A., C. Xin, A. K. Brust, V. A. Briner, and J. Pfeilschifter. 2004. Differential binding of ceramide to MEKK1 in glomerular endothelial and mesangial cells. *Biochim. Biophys. Acta.* 1636: 159-168.

Ikonen, E., and M. Jansen. 2008. Cellular sterol trafficking and metabolism: spotlight on structure. *Curr. Opin. Cell Biol*. 20: 371-377.

Israelachvili, J. 1991. *Intermolecular and surface forces*. Academic Press, San Diego.

Jaikishan, S., and J. P. Slotte. 2011. Effect of hydrophobic mismatch and interdigitation on sterol/sphingomyelin interaction in ternary bilayer membranes. *Biochim. Biophys. Acta*. 1808: 1940-1945.

Jaikishan, S., and J. P. Slotte. 2013. Stabilization of sphingomyelin interactions by interfacial hydroxyls - a study of phytosphingomyelin properties. *Biochim. Biophys. Acta*. 1828: 391-397.

Janiak, M. J., D. M. Small, and G. G. Shipley. 1979. Temperature and compositional dependence of the structure of hydrated dimyristoyl lecithin. *J. Biol. Chem.* 254: 6068-6078.

Janosi, L., and A. Gorfe. 2010. Importance of the sphingosine base double-bond geometry for the structural and thermodynamic properties of sphingomyelin bilayers. *Biophys. J.* 99: 2957-2966.

Jendrasiak, G. L., and R. L. Smith. 2001. The effect of the choline head group on phospholipid hydration. *Chem. Phys. Lipids.* 113: 55-66.

Jimenez-Rojo, N., A. B. Garcia-Arribas, J. Sot, A. Alanso, and F. M. Goni. 2014. Lipid bilayers containing sphingomyelins and ceramides of varying N-acyl lengths: a glimpse into sphingolipid complexity. *Biochim. Biophys. Acta*. 1838: 456-464.

Kahya, N., D. Scherfeld, K. Bacia, B. Poolman, and P. Schwille. 2003. Probing Lipid Mobility of Raft-exhibiting Model Membranes by Fluorescence Correlation Spectroscopy. *J. Biol. Chem.* 278: 28109-28115.

Kaiser, R. D., and E. London. 1998. Location of diphenylhexatriene (DPH) and its derivatives within membranes: comparison of different fluorescence quenching analyses of membrane depth. *Biochemistry*. 37: 8180-8190.

Kinoshita, M., N. Matsumori, and M. Murata. 2014. Coexistence of two liquid crystalline phases in dihydrosphingomyelin and dioleoylphosphatidylcholine binary mixtures. *Biochim. Biophys. Acta*. 1838: 1372-1381.

Kolesnick, R. N., F. M. Goni, and A. Alonso. 2000. Compartmentalization of ceramide signaling: physical foundations and biological effects. *J. Cell Physiol.* 184: 285-300.

Kooijman, E. E., J. Sot, L. R. Montes, A. Alonso, A. Gericke, B. Kruijff, S. Kumar, and F. M. Goni. 2008. Membrane organization and ionization behavior of the minor but crucial lipid ceramide-1-phosphate. *Biophys. J.* 94: 4320-4330.

Kooijman, E. E., V. Chupin, N. L. Fuller, M. M. Kozlov, B. de Kruijff, K. N. Burger, and P. R. Rand. 2005. Spontaneous curvature of phosphatidic acid and lysophosphatidic acid. *Biochemistry.* 44: 2097-2102.

Koynova, R., and M. Caffrey. 1995. Phases and phase transitions of the sphingolipids. *Biochim. Biophys. Acta.* 1255: 213-236.

Koynova, R., and M. Caffrey. 1998. Phases and phase transitions of the phosphatidylcholines. *Biochim. Biophys. Acta.* 1376: 91-145.

Kucerka, N., J. Pencer, J. N. Sachs, J. F. Nagle, and J. Katsaras. 2007. Curvature effect on the structure of phospholipid bilayers. *Langmuir.* 23: 1292-1299.

Kullberg, A., O. Ekholm, and J. P. Slotte. 2015. Miscibility of Sphingomyelins and Phosphatidylcholines in Unsaturated Phosphatidylcholine Bilayers. *Biophys. J.* 109: 1907-1916.

Kurinna, S. M., C. C. Tsao, A. F. Nica, T. Jiffar, and P. P. Ruvolo. 2004. Ceramide promotes apoptosis in lung cancer-derived A549 cells by a mechanism involving c-Jun NH2-terminal kinase. *Cancer Res*. 64: 7852-7856.

Lande, M. B., J. M. Donovan, and M. L. Zeidel. 1995. The relationship between membrane fluidity and permeabilities to water, solutes, ammonia, and protons. *J. Gen. Physiol.* 106: 67-84.

Lange, Y. 1991. Disposition of intracellular cholesterol in human fibroblasts. *J. Lipid Res.* 32: 329-339.

Laouini1, A., C. Jaafar-Maalej, I. Limayem-Blouza, S. Sfar, C. Charcosset, and H. Fessi1. 2012. Preparation, Characterization and Applications of Liposomes: State of the Art. *J. Colloid Science and Biotechnology*. 1: 147-168.

Laviad, E. L., L. Albee, I. Pankova-Kholmyansky, S. Epstein, H. Park, A. H. Merrill, Jr., and A. H. Futerman. 2008. Characterization of ceramide synthase 2: tissue distribution, substrate specificity, and inhibition by sphingosine 1-phosphate. *J. Biol. Chem.* 283: 5677-5684.

Lehtonen, J. Y., J. M. Holopainen, and P. K. Kinnunen. 1996. Evidence for the Formation of Microdomains in Liquid Crystalline Large Unilamellar Vesicles Caused by Hydrophobic Mismatch of the Constituent Phospholipids. *Biophys. J.* 70: 1753-1760.

Leventis, P. A., and S. Grinstein. 2010. The Distribution and Function of Phosphatidylserine in Cellular Membranes. *Annu. Rev. Biophys*. 2010. 39: 407-427.

Levy, M., and A. H. Futerman. 2010. Mammalian ceramide synthases. *IUBMB. Life.* 62: 347-356.

Li, L., X. Tang, K. G. Taylor, D. B. DuPre, and M. C. Yappert. 2002. Conformational characterization of ceramides by nuclear magnetic resonance spectroscopy. *Biophys. J.* 82: 2067-2080.

Li, Z., E. Mintzer, and R. Bittman. 2004. The critical micelle concentrations of lysophosphatidic acid and sphingosylphosphorylcholine. *Chem. Phys. Lipids* 130: 197-201.

Litman, B. J., E. N. Lewis, and I. W. Levin. 1991. Packing characteristics of highly unsaturated bilayer lipids: Raman spectroscopic studies of multilamellar phosphatidylcholine dispersions. *Biochemistry*. 30: 313-319.

Lofgren, H., and I. Pascher. 1977. Molecular arrangements of sphingolipids. The monolayer behaviour of ceramides. *Chem. Phys. Lipids*. 20: 273-284.

Lonnfors, M., J. P. Doux, J. A. Killian, T. K. M. Nyholm, and J. P. Slotte. 2011. Sterols have higher affinity for sphingomyelin than for phosphatidylcholine bilayers even at equal acyl-chain order. *Biophys. J.* 100: 2633-2641.

Luckey, M. 2008. *Membrane Structural Biology: With Biochemical and Biophysical Foundations*. Cambridge University Press, Cambridge, UK.

MacDonald, R. C., R. I. MacDonald, B. P. Menco, K. Takeshita, N. K. Subbarao, and L. R. Hu. 1991. Small-volume extrusion apparatus for preparation of large, unilamellar vesicles. *Biochim. Biophys. Acta.* 1061: 297-303.

Marrink, S. J., A. H. De Vries, and D. P. Tieleman. 2009. Lipids on the move: simulations of membrane pores, domains, stalks and curves. *Biochim. Biophys. Acta*. 1788: 149-168.

Marsh, D. 1996. Lateral pressure in membranes. *Biochim. Biophys. Acta.* 1286: 183-223.

Marsh, D. 1999. Thermodynamic analysis of chain-melting transition temperatures for monounsaturated phospholipid membranes: dependence on cis-monoenoic double bond position. *Biophys. J.* 77: 953-963.

Marsh, D. 2009. Cholesterol-induced fluid membrane domains: a compendium of lipid-raft ternary phase diagrams. *Biochim. Biophys. Acta*. 1788: 2114-2123.

Massey, J. B. 2001. Interaction of ceramides with phosphatidylcholine, sphingomyelin and sphingomyelin/cholesterol bilayers. *Biochim. Biophys. Acta.* 1510: 167-184.

Mathias, S., L. A. Pena, and R. N. Kolesnick. 1998. Signal transduction of stress via ceramide. *Biochem. J.* 335: 465-480.

Matsumori, N., T. Yasuda, H. Okazaki, T. Suzuki, T. Yamaguchi, H. Tsuchikawa, M. Doi, T Oishi and M. Murata. 2012. Comprehensive molecular motion capture for sphingomyelin by site-specific deuterium labeling. *Biochemistry*. 51: 8363-8370.

Maula, T., M. Kurita, S. Yamaguchi, T. Yamamoto, S. Katsumura, and J. P. Slotte. 2011. Effects of sphingosine 2N and 3O-methylation on palmitoyl ceramide properties in bilayer membranes. *Biophys. J.* 101: 2948-2956.

Maula, T., I. Artetxe, P. M. Grandell, and J. P. Slotte. 2012. Importance of the sphingoid base length for the membrane properties of ceramides. *Biophys. J.* 103: 1870-1879.

Maulucci, G., S. M. De, G. Arcovito, F. Boffi, A. C. Castellano, and G. Briganti. 2005. Particle size distribution in DMPC vesicles solutions undergoing different sonication times. *Biophys. J.* 88: 3545-3550.

Maxfield, F. R., and G. van, Meer. 2010. Cholesterol, the central lipid of mammalian cells. *Curr. Opin. Cell Biol*. 22: 422-429.

Mayer, L. D., M. J. Hope, and P. R. Cullis. 1986. Vesicles of variable sizes produced by a rapid extrusion procedure. *Biochim. Biophys. Acta.* 858: 161-168.

McMullen, T. P., C. Vilchèze, R. N. McElhaney, and R. Bittman. 1995. Differential scanning calorimetric study of the effect of sterol side chain length and structure on dipalmitoylphosphatidylcholine thermotropic phase behavior. *Biophys. J.* 69: 169-176.

Megha, and E. London. 2004. Ceramide selectively displaces cholesterol from ordered lipid domains (rafts): implications for lipid raft structure and function. *J. Biol. Chem.* 279: 9997-10004.

Megha, P. Sawatzki, T. Kolter, R. Bittman, and E. London. 2007. Effect of ceramide N-acyl chain and polar headgroup structure on the properties of ordered lipid domains (lipid rafts). *Biochim. Biophys. Acta*. 1768: 2205-2212.

Merrill, A. H., Jr., D. W. Nixon, and R. D. Williams. 1985. Activities of serine palmitoyltransferase (3-ketosphinganine synthase) in microsomes from different rat tissues. *J. Lipid Res.* 26: 617-622.

Merrill, A. H., Jr., E. Wang, and R. E. Mullins. 1988. Kinetics of long-chain (sphingoid) base biosynthesis in intact LM cells: effects of varying the extracellular concentrations of serine and fatty acid precursors of this pathway. *Biochemistry.* 27: 340-345.

Mizutani, Y., A. Kihara, and Y. Igarashi. 2005. Mammalian Lass6 and its related family members regulate synthesis of specific ceramides. *Biochem. J.* 390: 263-271.

Mizutani, Y., A. Kihara, and Y. Igarashi. 2006. LASS3 (longevity assurance homologue 3) is a mainly testis-specific (dihydro) ceramide synthase with relatively broad substrate specificity. *Biochem. J.* 398: 531-538.

Mizutani, Y., A. Kihara, H. Chiba, H. Tojo, and Y. Igarashi. 2008. 2-Hydroxy-ceramide synthesis by ceramide synthase family: enzymatic basis for the preference of FA chain length. *J. Lipid Res.* 49: 2356-2364.

Montes, L. R., D. J. Lopez, J. Sot, L. A Bagatolli, M. J. Stonehouse, M. L Vasil, B. X. Wu, Y. A. Hannun, F. M Goni, and A. Alonso. 2008. Ceramide-enriched membrane domains in red blood cells and the mechanism of sphingomyelinase-induced hot-cold hemolysis. *Biochemistry*. 47: 11222-11230.

Morad, S. A. F., and M. C. Cabot. 2013. Ceramide-orchestrated signalling in cancer cells. *Nat. Rev. Cancer*. 13: 51-65.

Mullen, T. D., Y. A. Hannun, and L. M. Obeid. 2012. Ceramide synthases at the centre of sphingolipid metabolism and biology. *Biochem. J.* 441: 789-802.

Muller, G., M. Ayoub, P. Storz, J. Rennecke, D. Fabbro, and K. Pfizenmaier. 1995. PKC zeta is a molecular switch in signal transduction of TNF-alpha, bifunctionally regulated by ceramide and arachidonic acid. *EMBO. J.* 14: 1961-1969.

Nagano, H., T. Nakanishi, H. Yao, and K. Ema. 1995. Effect of vesicle size on the heat capacity anomaly at the gel to liquid-crystalline phase transition in unilamellar vesicles of dimyristoylphosphatidylcholine. *Phys. Rev. E. Stat. Phys. Plasmas. Fluids Relat Interdiscip. Topics.* 52: 4244-4250.

Niemela, P., M. T. Hyvonen, and I. Vattulainen. 2004. Structure and dynamics of sphingomyelin bilayer: insight gained through systematic comparison to phosphatidylcholine. *Biophys. J.* 87: 2976-2989.

Nordlund, J. R., C. F. Schmidt, S. N. Dicken, and T. E. Thompson. 1981. Transbilayer distribution of phosphatidylethanolamine in large and small unilamellar vesicles. *Biochemistry.* 20: 3237-3241.

Norlen, L., I. Plasencia, and L. Bagatolli. 2008. Stratum corneum lipid organization as observed by atomic force, confocal and two-photon excitation fluorescence microscopy. *Int. J. Cosmet. Sci*. 30: 391-411.

Nurminen, T. A., J. M. Holopainen, H. Zhao, and P. K. Kinnunen. 2002. Observation of topical catalysis by sphingomyelinase coupled to microspheres. *J. Am. Chem. Soc*. 124: 12129-12134.

Nybond, S., Y. J. Bjorkqvist, B. Ramstedt, and J. P. Slotte. 2005. Acyl chain length affects ceramide action on sterol/sphingomyelin-rich domains. *Biochim. Biophys. Acta.* 1718: 61-66.

Nyholm, T. K., D. Lindroos, B. Westerlund, and J. P. Slotte. 2011. Construction of a DOPC/PSM/cholesterol phase diagram based on the fluorescence properties of trans-parinaric acid. *Langmuir*. 27: 8339-8350.

Nystrom, J. H., M. Lonnfors, and T. K. Nyholm. 2010. Transmembrane peptides influence the affinity of sterols for phospholipid bilayers. *Biophys. J.* 99: 526-533.

Obeid, L. M., C. M. Linardic, L. A. Karolak, and Y. A. Hannun. 1993. Programmed cell death induced by ceramide. *Science.* 259: 1769-1771.

O'Brien, J. S., and G. Rouser. 1964. The fatty acid composition of brain sphingolipids: sphingomyelin, ceramide, cerebroside, and cerebroside sulfate. *J. Lipid Res.* 5: 339-342.

Okazaki, T., R. M. Bell, and Y. A. Hannun. 1989. Sphingomyelin turnover induced by vitamin D3 in HL-60 cells. Role in cell differentiation. *J. Biol. Chem.* 264: 19076-19080.

Pandit, S. A., and H. L. Scott. 2006. Molecular-dynamics simulation of a ceramide bilayer. *J. Chem. Phys*. 124: 14708-14715.

Pascher, I. 1976. Molecular arrangements in sphingolipids. Conformation and hydrogen bonding of ceramide and their implication on membrane stability and permeability. *Biochim. Biophys. Acta.* 455: 433-451.

Pencer, J., A. Jackson, N. Kucerka, M. P. Nieh, and J. Katsaras. 2008. The influence of curvature on membrane domains. *Eur. Biophys. J.* 37: 665-671.

Pick, L., and M. Bielschowsky. 1927. Verhandlungen ärztlicher gesellschaften. *Klin. Wochenschr*. 6: 1631-1637.

Pieter, R. C., M. J. Hope, and C. P. S. Tilcock. 1986. Lipid polymorphism and the roles of lipids in membranes. *Chem. Phys. Lipids*. 40: 127-144.

Pike, L. J. 2006. Rafts defined: a report on the Keystone Symposium on Lipid Rafts and Cell Function. *J. Lipid Res.* 47: 1597-1598.

Pinto, S. N., L. C. Silva, R. F. de Almeida, and M. Prieto. 2008. Membrane domain formation, interdigitation, and morphological alterations induced by the very long chain asymmetric C24:1 ceramide. *Biophys. J.* 95: 2867-2879.

Pinto, S. N., L. C. Silva, A. H. Futerman, and M. Prieto. 2011. Effect of ceramide structure on membrane biophysical properties: the role of acyl chain length and unsaturation. *Biochim. Biophys. Acta.* 1808: 2753-2760.

Pinto, S. N., F. Fernandes, A. Fedorov, A. H. Futerman, L. C. Silva, and M. Prieto. 2013. A combined fluorescence spectroscopy, confocal and 2-photon microscopy approach to re-evaluate the properties of sphingolipid domains. *Biochim. Biophys. Acta.* 1828: 2099-2110.

Pruett, S. T., A. Bushnev, K. Hagedorn, M. Adiga, C. A. Haynes, M. C. Sullards, D. C. Liotta, and A. H. Merrill. 2008. Biodiversity of sphingoid bases ("sphingosines") and related amino alcohols. *J. Lipid Res.* 49: 1621-1639.

Pruschy, M., H. Resch, Y. Q. Shi, N. Aalame, C. Glanzmann, and S. Bodis. 1999. Ceramide triggers p53-dependent apoptosis in genetically defined fibrosarcoma tumour cells. *Br. J. Cancer*. 80: 693-698.

Ramstedt, B., and J. P. Slotte. 2002. Membrane properties of sphingomyelins. *FEBS Lett*. 531: 33-37.

Rawicz, W., B. A Smith, T. J. McIntosh, S. A. Simon, and E. Evans. 2008. Elasticity, Strength, and Water Permeability of Bilayers that Contain Raft Microdomain-Forming Lipids. *Biophys. J.* 94: 4725-4736.

Rerek, M. E., H. Chen, B. Markovic, D. Van Wyck, P.Garidel, R. Mendelsohn, and D. J. Moore. 2001. Phytosphingosine and sphingosine ceramide headgroup hydrogen bonding: structural insights through thermotropic hydrogen/deuterium exchange. *J. Phys. Chem*. 105: 9355-9362.

Reynolds, C. P., B. J. Maurer, and R. N. Kolesnick. 2004. Ceramide synthesis and metabolism as a target for cancer therapy. *Cancer Lett*. 206: 169-180.

Richardson, E. S., W. G. Pitt, and D. J. Woodbury. 2007. The role of cavitation in liposome formation. *Biophys. J.* 93: 4100-4107.

Riebeling, C., J. C. Allegood, E. Wang, A. H. Merrill, Jr., and A. H. Futerman. 2003. Two mammalian longevity assurance gene (LAG1) family members, trh1 and trh4, regulate dihydroceramide synthesis using different fatty acyl-CoA donors. *J. Biol. Chem.* 278: 43452-43459.

Roux, A., D. Cuvelier, P. Nassoy, J. Prost, P. Bassereau, and B. Goud. 2005. Role of curvature and phase transition in lipid sorting and fission of membrane tubules. *EMBO. J.* 24: 1537-1545.

Ruiz-Arguello, M. B., G. Basanez, F. M. Goni, and A. Alonso. 1996. Different effects of enzymegenerated ceramides and diacylglycerols in phospholipid membrane fusion and leakage. *J. Biol. Chem.* 271: 26616-26621.

Ruiz-Arguello, M. B., F. M. Goni, and A. Alonso. 1998. Vesicle membrane fusion induced by the concerted activities of sphingomyelinase and phospholipase C. *J. Biol. Chem*. 273: 22977-22982.

Sandhoff, R. 2010. Very long chain sphingolipids: tissue expression, function and synthesis. *FEBS Lett*. 584: 1907-13.

Scheidt, H. A., P. Muller, A. Herrmann, and D. Huster. 2003. The potential of fluorescent and spin-labeled steroid analogs to mimic natural cholesterol. *J. Biol. Chem.* 278: 45563-45569.

Sessa, G., and G. Weissmann. 1968. Phospholipid spherules (liposomes) as a model for biological membranes. *J. Lipid Res.* 9: 310-318.

Shah, J., J. M. Atienza, R. I. Duclos, Jr., A. V. Rawlings, Z. Dong, and G. G. Shipley. 1995. Structural and thermotropic properties of synthetic C16:0 (palmitoyl) ceramide: effect of hydration. *J. Lipid Res.* 36: 1936-1944.

Shaikh, S. R., D. S. Locascio, S. P. Soni, S. R. Wassall, and W. Stillwell. 2009. Oleic- and docosahexaenoic acid-containing phosphatidylethanolamines differentially phase separate from sphingomyelin. *Biochim. Biophys. Acta*. 1788: 2421-2426.

Silva, L. C., R. F. de Almeida, A. Fedorov, A. P. Matos, and M. Prieto. 2006. Ceramide-platform formation and -induced biophysical changes in a fluid phospholipid membrane. *Mol. Membr. Biol*. 23: 137-148.

Silva, L. C., R. F. de Almeida, B. M. Castro, A. Fedorov, and M. Prieto. 2007. Ceramide-domain formation and collapse in lipid rafts: membrane reorganization by an apoptotic lipid. *Biophys. J.* 92: 502-516.

Silva, L. C., A. H. Futerman, and M. Prieto. 2009. Lipid raft composition modulates sphingomyelinase activity and ceramide-induced membrane physical alterations. *Biophys. J.* 96: 3210-3222.

Simons, K., and E. Ikonen. 1997. Functional rafts in cell membranes. *Nature*. 387: 569-572.

Simons, K., and D. Toomre. 2000. Lipid rafts and signal transduction. *Nat. Rev. Mol. Cell Biol.* 1: 31-39.

Simons, K., and R. Ehehalt. 2002. Cholesterol, lipid rafts, and disease. *J. Clin. Invest*. 110: 597-603.

Singer, S. J., and G. L. Nicolson. 1972. The fluid mosaic model of the structure of cell membranes. *Science.* 175: 720-731.

Sklar, L. A., G. P. Miljanich, and E. A. Dratz. 1979. Phospholipid lateral phase separation and the partition of cis-parinaric acid and trans-parinaric acid among aqueous, solid lipid, and fluid lipid phases. *Biochemistry*. 18: 1707-1716.

Slotte J. P., T. Yasuda T, O. Engberg, Al Sazzad M. A., V. Hautala, T. K. M. Nyholm, and M. Murata. 2017. Bilayer Interactions among Unsaturated Phospholipids, Sterols, and Ceramide. *Biophys. J*. 112: 1673-1681.

Slotte, J. P. 2013. Biological functions of sphingomyelins. *Prog. Lipid Res*. 52: 424-437.

Soni, S. P., D. S Locascio, Y. Liu, J. A. Williams, R. Bittman, W. Stillwell, and S. R. Wassall. 2008. Docosahexaenoic acid enhances segregation of lipids between: 2H-NMR study. *Biophys. J.* 95: 203-214.

Sot, J., F. J. Aranda, M. I. Collado, F. M. Goni, and A. Alonso. 2005. Different effects of long- and short-chain ceramides on the gel-fluid and lamellar-hexagonal transitions of phospholipids: a calorimetric, NMR, and x-ray diffraction study. *Biophys. J.* 88: 3368-3380.

Sot, J., L. A. Bagatolli, F. M. Goni, and A. Alonso. 2006. Detergent-resistant, ceramide-enriched domains in sphingomyelin/ceramide bilayers. *Biophys. J*. 90: 903-914.

Spiegel, S., D. Foster, and R. Kolesnick. 1996. Signal transduction through lipid second messengers. *Curr. Opin. Cell Biol*. 8: 159-167.

Stancevic, B., and R. Kolesnick. 2010. Ceramide-rich platforms in transmembrane signaling. *FEBS Lett*. 584: 1728-1740.

Staneva, G., A. Momchilova, C. Wolf, P. J. Quinn, and K. Koumanov. 2009. Membrane microdomains: role of ceramides in the maintenance of their structure and functions. *Biochim. Biophys. Acta.* 1788: 666-675.

Szoka, F., and D. Papahadjopoulos. 1980. Comparative properties and methods of preparation of lipid vesicles (liposomes). *Annu. Rev. Biophys. Bioeng*. 9: 467-508.

Talbott, C. M., I. Vorobyov, M. C. Yappert. 2000. Conformational studies of sphingolipids by NMR spectroscopy. II. Sphingomyelin. *Biochim. Biophys. Acta*. 1467: 326-337.

Tenchov, B., and R. Koynova. 2012. Cubic phases in membrane lipids. *Eur. Biophys. J.* 41: 841-850.

Thomas, R. L., C. M. Matsko, M. T. Lotze, and A. A. Amoscato. 1999. Mass spectrometric identification of increased C16 ceramide levels during apoptosis. *J. Biol. Chem*. 274: 30580-30588.

Thudicum, J. L. W. 1884. *A treatise on the chemical constitution of brain*. Bailliere, Tindall and Cox, London

Trajkovic, K., C. Hsu, S. Chiantia, L. Rajendran, D. Wenzel, F. Wieland, P. Schwille, B. Brugger, and M. Simons. 2008. Ceramide triggers budding of exosome vesicles into multivesicular endosomes. *Science.* 319: 1244-1247.

van Holde, K. E., W. C. Johnson, and P. S. Ho. 1998. *Principles of physical Biochemistry*. Prentice-Hall, Inc., New Jersey.

van Meer, G. 2005. Cellular lipidomics. *EMBO. J*. 24: 3159-3165.

van Meer, G., D. R. Voelker, and G. W. Feigenson. 2008. Membrane lipids: where they are and how they behave. *Nat. Rev. Mol. Cell Biol*. 9: 112-124.

van Smeden, J., M. Janssens, G. S. Gooris, and J. A. Bouwstra. 2013. The Important Role of Stratum Corneum Lipids for the Cutaneous Barrier Function. *Biochim. Biophys. Acta*. 1841: 295-313.

Veiga, M. P., J. L. Arrondo, F. M. Goni, and A. Alonso. 1999. Ceramides in phospholipid membranes: effects on bilayer stability and transition to nonlamellar phases. *Biophys. J.* 76: 342-350.

Venkataraman, K., C. Riebeling, J. Bodennec, H. Riezman, J. C. Allegood, M. C. Sullards, A. H. Merrill, Jr., and A. H. Futerman. 2002. Upstream of growth and differentiation factor 1 (uog1), a mammalian homolog of the yeast longevity assurance gene 1 (LAG1), regulates N-stearoylsphinganine (C18-(dihydro) ceramide) synthesis in a fumonisin B1-independent manner in mammalian cells. *J. Biol. Chem.* 277: 35642-35649.

Vist, M. R., and J. H. Davis. 1990. Phase equilibria of cholesterol/dipalmitoylphosphatidylcholine mixtures: 2H nuclear magnetic resonance and differential scanning calorimetry. *Biochemistry.* 29: 451-464.

Wang, T. Y., and J. R. Silvius. 2003. Sphingolipid partitioning into ordered domains in cholesterol free and cholesterol-containing lipid bilayers. *Biophys. J.* 84: 367-378.

Watson, P., and D. J. Stephens. 2005. ER-to-Golgi transport: form and formation of vesicular and tubular carriers. *Biochim. Biophys. Acta.* 1744: 304-315.

Westerlund, B., P. M. Grandell, Y. J. Isaksson, and J. P. Slotte. 2010. Ceramide acyl chain length markedly influences miscibility with palmitoyl sphingomyelin in bilayer membranes. *Eur. Biophys. J.* 39: 1117-1128.

Williams, J. A., S. E. Batten, M. Harris, B. D. Rockett, S. R. Shaikh, W. Stillwell, and S. R. Wassall. 2012. Docosahexaenoic and eicosapentaenoic acids segregate differently between raft and nonraft domains. *Biophys. J.* 103: 228-237.

Williams, R. D., E. Wang, and A. H. Merrill. 1984. Enzymology of long-chain base synthesis by liver: characterization of serine palmitoyltransferase in rat liver microsomes. *Arch. Biochem. Biophys*. 228: 282-291.

Wu BX, C. J. Clarke, and Y. A. Hannun. 2010. Mammalian neutral sphingomyelinases: regulation and roles in cell signaling responses. *Neuromol. Med*. 12: 320-330.

Yamaoka, S., M. Miyaji, T. Kitano, H. Umehara, and T. Okazaki. 2004. Expression cloning of a human cDNA restoring sphingomyelin synthesis and cell growth in sphingomyelin synthase-defective lymphoid cells. *J. Biol. Chem*. 279: 18688-18693.

Yeagle, P. L. 2005. *The structure of biological membranes*. CRC Press, Boca Raton, FL.

Zhang, J., N. Alter, J. C. Reed, C. Borner, L. M. Obeid, and Y. A. Hannun. 1996. Bcl-2 interrupts the ceramide-mediated pathway of cell death. *Proc. Natl. Acad. Sci. U S A*. 93: 5325-5328.

Zhang, Y., B. Yao, S. Delikat, S. Bayoumy, Lin XH, S. Basu, M. McGinley, P. Chan-Hui, H. Lichenstein and R. Kolesnick. 1997. Kinase suppressor of Ras is ceramide-activated protein kinase. *Cell.* 89: 63-72.

Zheng, W., J. Kollmeyer, H. Symolon, A Momin, E. Munter, E. Wang, S. Kelly, J. Allegood, Y. Liu, Q. Peng, H. Ramaraju, M. Sullards, M. Cabot, and A. H. Merrill. 2006. Ceramides and other bioactive sphingolipid backbones in health and disease: lipidomic analysis, metabolism and roles in membrane structure, dynamics, signaling and autophagy. *Biochim. Biophys. Acta.*1758: 1864-84.

The Author

Md. Abdullah Al Sazzad received his BSc in Biotechnology and Genetic Engineering from Khulna University, Bangladesh. He completed his MSc in Bioinformatics from University of Turku in 2013. His PhD thesis project has taken place during October, 2013 – December, 2017 in Biochemistry, Faculty of Science and Engineering, Åbo Akademi University, Finland.

ISBN 978-952-12-3614-3